

## GEL DNA

### A Cloning-and Polymerase Chain Reaction-Free Method for CRISPR-Based Multiplexed Genome Editing

Randazzo, Paola; Bennis, Nicole Xanthe; Daran, Jean Marc; Daran-Lapujade, Pascale

#### DOI

[10.1089/crispr.2020.0028](https://doi.org/10.1089/crispr.2020.0028)

#### Publication date

2021

#### Document Version

Accepted author manuscript

#### Published in

CRISPR Journal

#### Citation (APA)

Randazzo, P., Bennis, N. X., Daran, J. M., & Daran-Lapujade, P. (2021). GEL DNA: A Cloning-and Polymerase Chain Reaction-Free Method for CRISPR-Based Multiplexed Genome Editing. *CRISPR Journal*, 4(6), 896-913. <https://doi.org/10.1089/crispr.2020.0028>

#### Important note

To cite this publication, please use the final published version (if applicable). Please check the document version above.

#### Copyright

Other than for strictly personal use, it is not permitted to download, forward or distribute the text or part of it, without the consent of the author(s) and/or copyright holder(s), unless the work is under an open content license such as Creative Commons.

#### Takedown policy

Please contact us and provide details if you believe this document breaches copyrights. We will remove access to the work immediately and investigate your claim.


# gEL DNA, a cloning- and PCR-free method for CRISPR-based multiplexed genome editing

Paola Randazzo<sup>1</sup>, Nicole Xanthe Bennis<sup>1</sup>, Jean-Marc Daran<sup>1</sup>, Pascale Daran-Lapujade<sup>1,#</sup>

<sup>1</sup> Department of Biotechnology, Delft University of Biotechnology, van der Maasweg 9, 2629HZ Delft, The Netherlands

# Corresponding author

 [p.a.s.daran-lapujade@tudelft.nl](mailto:p.a.s.daran-lapujade@tudelft.nl)

 +31 15 278 9965

## Keywords

Cas12a, T7 RNA polymerase, multiplex genome editing, cloning-free editing, yeast

## Abstract

Even for the genetically accessible yeast *Saccharomyces cerevisiae*, the CRISPR/Cas DNA editing technology has strongly accelerated and facilitated strain construction. Several methods have been validated for fast and highly efficient single editing events and diverse approaches for multiplex genome editing have been described in literature by means of *SpCas9* or *FnCas12a* endonucleases and their associated gRNAs. The gRNAs used to guide the Cas endonuclease to the editing site are typically expressed from plasmids using native PolIII or PolIII RNA polymerases. These gRNA-expression plasmids require laborious, time-consuming cloning steps, which hampers their implementation for academic and applied purposes. In this study, we explore the potential of expressing gRNA from linear DNA fragments using the T7 RNA polymerase (T7RNAP) for single and multiplex genome editing in *S. cerevisiae*. Using *FnCas12a*, this work demonstrates that transforming short, linear DNA fragments encoding gRNAs in yeast strains expressing T7RNAP promotes highly efficient single and duplex DNA editing. These DNA fragments can be custom-ordered, which makes this approach highly suitable for high-throughput strain construction. This work expands the CRISPR-toolbox for large-scale strain construction programs in *S. cerevisiae* and promises to be relevant for other, less genetically accessible yeast species.

## Introduction

The bacterial-derivative CRISPR-Cas technology is nowadays the most commonly used tool for microbial genome engineering. For the eukaryotic model and industrial workhorse *Saccharomyces cerevisiae*, several CRISPR-based methodologies have been developed aiming at fast and efficient single editing event.<sup>1-4</sup> Two Class II bacterial endonucleases, Cas9 and Cas12a (also known as Cpf1) have been functionally characterized for DNA editing ranging from point mutation to heterologous pathway integration.<sup>4-6</sup> While diverse Cas9- and Cas12a-mediated approaches for multiplex genome editing have been described in literature (reviewed in <sup>7</sup>), multiplex genome editing still requires substantial efforts for the CRISPR tools to be built. The RNA molecules designed to guide the endonuclease towards the editing site (gRNAs) are typically cloned in and expressed from plasmids. In most published works so far, multiplex editing relies on the parallel transformation of multiple plasmids carrying a single or two gRNAs. However, this approach is limited by the number of available marker-based plasmid backbones.<sup>4,8-12</sup> More recently, several successful examples have shown that several gRNAs can be expressed from a single gRNA-array, using different tricks to release the mature gRNAs.<sup>3,5,6,13-17</sup> However, complexity of these gRNA expression cassettes and their tailored sequence design may be difficult to synthesize and requires laborious and time-consuming cloning steps, therefore hindering the workflow for strain construction. To date, few attempts have been developed to circumvent gRNA cloning for genome editing of microbes in general and of *S. cerevisiae* in particular (illustrated in Fig. 1).

The most straightforward, cloning-free strategy would rely on the delivery of the gRNA in the form of a short, linear DNA fragment. Such short DNA fragments could easily be synthesized as oligonucleotides and delivered as mixture in any desired gRNA combination for multiplex targeting of DNA sites. Such a cost-effective and versatile approach would be highly suited for high-throughput, multiplex genome engineering of strains. Transient expression of linear DNA carrying gRNA expression cassettes has been previously shown to enable Cas9-mediated DNA-editing.<sup>9,18</sup> However, these approaches systematically require a first *in vitro* step for the construction of vectors from which the linear DNA is produced by PCR amplification (Fig. 1). In eukaryotes, gRNAs are transcribed either by RNA polymerase III (RNAPolIII) or by RNA Polymerase II (RNAPolII) promoter, this latter being flanked by self-processing ribozymes or tRNAs that prevent unwanted processing of the gRNAs.<sup>16,17</sup> A recent report has shown that functional gRNAs can also be transcribed in different yeasts by the RNA polymerase from bacteriophage T7 (T7RNAP) localized in the nucleus.<sup>19</sup> Delivered as plasmid DNA, the T7RNAP-transcribed gRNAs have been used to guide Cas9 for genome editing and dCas9 for transcriptional regulation.

The present work introduces the gEL DNA method, a novel, utterly cloning and PCR-free genome editing tool, based on the gRNA Expression from short, Linear double-stranded DNA oligos by the T7RNAP (Fig. 2). Comparing *SpCas9* and *FnCas12a*, this study demonstrates that *FnCas12a* enables efficient single and multiplexed DNA editing from custom-ordered oligonucleotides of 87

nt in *S. cerevisiae*. Next to gRNA *in silico* design, the only steps required for genome editing are transformation and screening. Highly suited for high-throughput strain construction, the gEL DNA method does not require prior knowledge on the transcription machinery of the host microbe (e.g. RNA processing and promoters) and thereby promises to facilitate DNA editing in less genetically accessible microbes.

## Materials and Methods

### Strains and cultivation conditions

All *S. cerevisiae* strains used in this study (Table 1) were derived from the CEN.PK background strain.<sup>20</sup> Yeast cells were grown at 30 °C in shake flasks on rotary shaker (200 rpm) or on agar plates (20 g l<sup>-1</sup>). Complex medium contained 10 g l<sup>-1</sup> of yeast extract, 20 g l<sup>-1</sup> of peptone and 20 g l<sup>-1</sup> of glucose (YPD). YPD was supplemented with nourseothricin (100 mg l<sup>-1</sup>), geneticin (G418) (200 mg l<sup>-1</sup>) or hygromycin B (200 mg l<sup>-1</sup>) to select transformants. Minimal synthetic media were prepared as previously described.<sup>21</sup> SMD medium contained 5 g l<sup>-1</sup> of (NH<sub>4</sub>)<sub>2</sub>SO<sub>4</sub>, 3 g l<sup>-1</sup> of KH<sub>2</sub>PO<sub>4</sub>, 0.5 g l<sup>-1</sup> of MgSO<sub>4</sub>·7H<sub>2</sub>O, 1 ml l<sup>-1</sup> of a trace element solution, supplemented with 20 g l<sup>-1</sup> of glucose and 1 ml l<sup>-1</sup> of a vitamin solution. SMD-urea included 6.6 g l<sup>-1</sup> K<sub>2</sub>SO<sub>4</sub>, 3.0 g l<sup>-1</sup> KH<sub>2</sub>PO<sub>4</sub>, 0.5 g l<sup>-1</sup> MgSO<sub>4</sub>·7H<sub>2</sub>O, 1 ml l<sup>-1</sup> trace elements solution, supplemented with 20 g l<sup>-1</sup> of glucose, 1 ml l<sup>-1</sup> of a vitamin solution and 2.3 g l<sup>-1</sup> CH<sub>4</sub>N<sub>2</sub>O.<sup>22</sup> Utilization of urea as nitrogen source instead of ammonium prevents excessive acidification of the medium resulting from ammonium uptake, and thereby enables to maintain the culture pH close to the initially set value. For selection of transformants carrying the *amdS* marker cassette, ammonium sulphate in SMD was substituted with 10 mM acetamide and 6.6 g l<sup>-1</sup> K<sub>2</sub>SO<sub>4</sub> (SM-Ac).<sup>23</sup> Plasmids were propagated in *Escherichia coli* XL1-Blue cells (Agilent Technologies, Santa Clara, CA), after growth in Lysogeny broth (LB; 10 g l<sup>-1</sup> tryptone, 5 g l<sup>-1</sup> yeast extract, 10 g l<sup>-1</sup> NaCl) liquid culture (180 rpm) or solid medium (20 g l<sup>-1</sup> agar) supplemented with chloramphenicol (25 mg l<sup>-1</sup>), spectinomycin (100 mg l<sup>-1</sup>) or ampicillin (100 mg l<sup>-1</sup>) at 37 °C. When required, plasmids from yeasts isolates were removed accordingly to described procedures.<sup>4</sup> All *S. cerevisiae* and *E. coli* stocks were prepared by aseptically adding 30% v/v of glycerol to exponentially growing cultures. Aliquoted cell stocks were stored at -80 °C.

### Molecular biology techniques

Yeast genomic DNA used for cloning purposes was isolated using the YeaStar genomic DNA kit (Zymo Research, Irvine, CA) according to manufacturer's instructions. Diagnostic PCR was performed using DreamTaq DNA polymerase (Thermo Fisher Scientific, Waltham, MA). For cloning and sequencing purposes, PCR products were obtained using Phusion<sup>®</sup> High-Fidelity DNA Polymerase (Thermo Fisher Scientific). Primers were ordered as PAGE or desalted purified oligonucleotides (Table S1) from Sigma-Aldrich (St Louis, MO). Annealed oligos were quantified by BR ds DNA kit using Qubit spectrophotometer (Invitrogen, Carlsbad, CA). DNA fragments were separated by electrophoresis on 1% (w/v) or 2% (w/v) agarose gels, depending on the fragment size. PCR products were purified using GenElute™ PCR Clean-Up Kit (Sigma-Aldrich), after restriction digestion of the PCR mixture with DpnI (Thermo Fisher Scientific) for removal of circular templates. When required, DNA fragments were excised from gel and purified using Zymoclean™ Gel DNA Recovery Kit (Zymo Research, Irvine, CA). Plasmids were isolated from *E. coli* cultures using Sigma GenElute™ Plasmid Miniprep kit (Sigma-Aldrich).

## Entry-vector plasmids construction

All plasmids used in this study are listed in Table 2.

The pUD565 plasmid<sup>24</sup>, a GFP dropout (GFPdo) entry vector compatible with Yeast Toolkit parts<sup>25</sup>, was ordered as synthetic gene from GeneArt (Thermo Fisher Scientific). GFPdo entry vectors for cloning of transcriptional unit were constructed following the BsaI Golden Gate reaction protocol described by Lee *et al.*<sup>25</sup>. The GFPdo pGGKd018 plasmid was obtained by assembly of part plasmids pYTK002, pYTK047, pYTK067, pYTK077, pYTK082, pYTK085. The GFPdo pGGKd034 plasmid was constructed by assembly of part plasmids pYTK002, pYTK047, pYTK067, pYTK079, pYTK082, pYTK083. The GFPdo pUDE810, an entry vector for *FnCas12a*-crRNAs, was constructed by Golden Gate assembly of pre-annealed primers 12647-12648 with the following PCR generated fragments: the pGGKd018 backbone with primers 12799-12800; the *SNR52* promoter amplified from the pMEL13 template<sup>4</sup> using primers 12645-13546; the GFPdo cassette bearing specific overhangs (GATC and ATCC) obtained by PCR amplification of primers 13547-12644 on pYTK047<sup>25</sup>.

## Construction of the dual Cas-expressing strain IMX1752

The construct for genomic integration of *Spcas9* gene consisted of a paired expression cassette for introduction of *Streptococcus pyogenes* *Spcas9* nuclease and *natNT2* marker into the *SGA1* locus.<sup>4</sup> First, the *natNT2* marker was PCR amplified from pUG-natNT2 (Addgene plasmid #110922<sup>26</sup>) using primers 10297 and 10298. This PCR product was cloned via Golden Gate together with pre-annealed primer pairs 10293-10294 and 10295-10296, and Yeast toolkit plasmids pYTK013, pYTK036, pYTK051, pYTK082, pYTK083<sup>25</sup>, resulting in plasmid pUDE483. The *SpCas9*-natNT2 integration cassette was obtained by enzyme restriction of pUDE483 using EcoRI. The restriction mix was directly transformed into *S. cerevisiae* using the lithium acetate (LiAc) transformation protocol.<sup>27</sup> Transformants were selected on YPD supplemented with nourseothricin. A single isolate, which was renamed IMX1714 (Table 1), was submitted to an additional transformation for the genomic integration of the *FnCas12a* nuclease. For this, the sequence of *Francisella novicida cas12a* was amplified from pUDC175 (Addgene plasmid #103019<sup>5</sup>) using primers 13553-13554. The obtained PCR product, carrying 60bp homology flanks to the X-2 integration site<sup>28</sup>, was transformed in IMX1714 as previously described in<sup>27</sup>, together with plasmid pUDR573<sup>29</sup> for *SpCas9*-mediated targeting at this genomic site. Transformants were selected on SM-Ac plates. Correct genomic integrations were confirmed by diagnostic PCR using primers listed in Table S1. After removal of the gRNA expression plasmid, the dual Cas9/Cas12a *S. cerevisiae* strain was stocked as IMX1752.

## Construction of the T7RNAP<sup>K276R</sup>-expressing strain IMX1905

First, the T7RNAP<sup>K276R</sup> sequence was PCR amplified from plasmid pRS315-nls-T7-RNAP (Addgene plasmid #33152)<sup>30</sup> using primers 13543 and 13544, and the obtained PCR fragment stably cloned into entry vector pUD565, resulting in part plasmid pGGKp172. The T7RNAP<sup>K276R</sup> transcriptional

unit was assembled by Golden Gate cloning into plasmid pGGKd034, together with part plasmids pGGKp035 (*TDH3p*) and pGGKp039 (*TEF1t*)<sup>24</sup>, leading to plasmid pUDE866.

For genomic integration of the T7RNAP<sup>K276R</sup>, the previously characterized YPRC $\tau$ 3 site of *S. cerevisiae* genome was chosen as recipient locus.<sup>31</sup> Thus, a gRNA for *FnCas12a*-mediated editing at this site was designed accordingly to guidelines provided in Swiat *et al.*<sup>5</sup> The gRNA for integration in YPRC $\tau$ 3 was ordered as oligos 14142-14143 containing specific overhangs for Golden Gate assembly (GATC and ATCC). Oligo annealing and cloning into pUDE810 plasmid resulted in the crRNA-expressing plasmid pUDR477. Amplification of the T7RNAP<sup>K276R</sup> integrative cassette was carried out on pUDE866 plasmid using primers 14022 and 14023, which contain repair ends of 60 bp homologous to the YPRC $\tau$ 3 locus. This generated PCR fragments were co-transformed with plasmid pUDR477 into IMX1752 cells, as previously described.<sup>27</sup> Yeast cells were selected on solid YPD plates supplemented with G418. Diagnostic PCR was performed on a single colony isolate, plasmid was recycled and the constructed strain was renamed IMX1905.

### Construction of T7RNAP mutants and T7RNAP-overexpressing strains

In order to alter the T7RNAP protein sequence, the *T7RNAP* gene of IMX1905 was *in vivo* mutated by means of the CRISPR-*SpCas9* editing machinery. A single gRNA was chosen for targeting the sequence surrounding DNA encoding amino acids at positions 266 and 276 (corresponding to 276 and 286 if considering the NLS) (Fig. S3). For this, oligo 14284 was Gibson assembled by bridging to the pMEL13<sup>4</sup> backbone, which was previously PCR amplified using primers 6005-6006. The obtained plasmid was renamed pUDR506. Repair oligos (Table S1) consist of 120-bp surrounding the T7RNAP targeted sequence with SNPs for P266L and/or R276K mutations, and carrying a silent mutation at the PAM sequence to avoid reiterative cutting. Plasmid pUDR506 and each double-stranded repair oligos were co-transformed into competent IMX1905 cells.<sup>27</sup> Transformants were plated on YPD agar supplemented with G418. Screening of eight selected colonies was performed by SNP genotyping with primers listed in Table S1, following previously described procedures for SNP scoring.<sup>32</sup> After SNPs validation and Sanger sequencing of the mutated T7RNAP sequence (Fig. S3), strains were stocked as follow: IMX2030 (T7RNAP<sup>P266L, K276R</sup>) was renamed after the P266L amino acid substitution; IMX2031 (*wt*T7RNAP) expresses the wild-type T7RNAP, where the arginine at position 276 is changed into the native lysine; IMX2032 (T7RNAP<sup>P266L</sup>) resulted from simultaneous mutations of proline and arginine at positions 266 and 277 for the respective amino acid change in leucine and lysine.

For the T7RNAP<sup>K276R</sup> overexpression, the dual Cas-expressing strain IMX1752 was transformed with plasmid pUDE866, following standard practice.<sup>27</sup> Transformants were selected on YPD plates supplemented with hygromycin B and the strain was renamed as IME459. In parallel, transformation of IMX1752 with the empty vector pGGKd034 led to the control strain IME460. To overexpress the T7RNAP<sup>P266L</sup> variant, the gene sequence of strain IMX2032 was PCR amplified from its isolated genomic DNA, using primers 10753 and 10768. The obtained PCR product was cloned by Golden Gate assembly into the episomal entry plasmid pGGKd034. The



obtained plasmid, renamed pUDE911, was therefore transformed into IMX1752, transformants plated on selective YPD hygromycin B medium and selected colonies stocked as IME475.

### Construction of the *FnCas12a-T7RNAP<sup>K276R</sup>* transportable system

To construct plasmids carrying *FnCas12a* expression cassettes, two alternative promoters were cloned by Golden Gate into the pGGKd034 vector together with the PCR product obtained by amplifying pUDC175 using primers 18075-18076. Plasmid pGGKp100 (PFK1p)<sup>33</sup> was used for assembly of pUDE1082, while plasmid pYTK027 (REV1p)<sup>25</sup> for the construction of pUDE1086. Cloning of the transportable *FnCas12a-T7RNAP<sup>K276R</sup>* system was performed by Gibson assembly using PCR amplicons with synthetic flags of 60 bp. Flagged primers 18077-18166 were used for PCR linearization of plasmid pUDE911. Flagged *FnCas12a* expression cassettes were amplified from pUDC175, pUDE1082 or pUDE1086 templates using primers 11868-10189, 18078-10189 or 18132-10189, respectively. Gibson assembly of these alternative *FnCas12a* expression cassettes to the linearized pUDE911 resulted in assembly of the respective plasmids pUDE1083, pUDE1084 and pUDE1087. CEN.PK113-7D transformed with each of the episomal plasmid were stocked as strains IME638 (pUDE911), IME639 (pUDE1082), IME640 (pUDE1083), IME641 (pUDE1084), IME642 (pGGKd034), IME645 (pUDE1086) and IME646 (pUDE1087). All transformants were selected on selective YPD hygromycin B medium.

### Assembly of gRNA expression cassettes

The gRNA cassettes for evaluation of *ADE2* deletion efficiencies mediated by *FnCas12a* or *SpCas9* nucleases were prepared using the highly-efficient *ADE2-3*<sup>5</sup> or the *ADE2.y*<sup>1</sup> gRNAs, respectively. Each gRNA cassette was expressed from high-copy plasmid and comprised the gRNA sequence left-flanked by the RNAPolIII-dependent *SNR52p*, the minimal *T7p* 'TAATACGACTCACTATA' (*S.T7p*) or an extended *T7p* 'GCCGGGAATTTAATACGACTCACTATA' (*L.T7p*), with respective terminator sequences at the right flank. For the *FnCas12a*-mediated targeting of other genes, previously characterized gRNAs were expressed as single gRNA-expressing cassette or as in an array-like arrangement: *HIS4* (*HIS4-4*), *PDR12* (*PDR12-3*) or *CAN1* (*CAN1-4* or *CAN1-3*).<sup>5</sup>

All single gRNA-expressing plasmids were assembled by Gibson assembly reaction using the NEBuilder® HiFi DNA Assembly Master Mix (New England Biolabs). Depending on the plasmid features, the backbone of the pUDE810 plasmid was amplified using different primer couples for specific homology overhangs. The backbone for assembly of *FnCas12a*-gRNAs with *SNR52p/SUP4t* flanks was obtained by PCR amplification with primers 12710-5793. For T7RNAP-mediated expression of gRNAs via *FnCas12a*, plasmid backbone was obtained by PCR amplification using either primers 14274-13713 (*S.T7p/T7t*) or 14275-13713 (*L.T7p/T7t*). Plasmid pUDE759 was assembled by *SNR52p/SUP4t* backbone fragment with annealed oligos 12713-12714. Single oligos were used for the Gibson assembly of *FnCas12a*-gRNAs cassettes by single-stranded DNA bridging to each individual PCR-originated backbone fragments: the *SNR52p/SUP4t* derivatives pUDR482 (primer 14282), pUDR483 (primer 13750), pUDR484 (primer 14283), pUDR715 (primer 17328), pUDR716 (primer 17329), pUDR717 (primer 17330), pUDR718

(primer 17331); the *S.T7p/T7t*-related plasmids pUDR485 (primer 14280), pUDR486 (primer 13751), pUDR487 (primer 14281), pUDR488 (primer 13572); the *L.T7p/T7t* cognate plasmids pUDR489 (primer 14276), pUDR490 (primer 14277), pUDR491 (primer 14278) and pUDR492 (primer 14279).

For assembly of *SpCas9*-gRNAs under *SNR52p*, the amplified pUDE810 backbone with *SNR52p/SUP4t* edges was mixed with annealed oligos 15508-15509 and the single-stranded oligo 14426 in a Gibson reaction, resulting in plasmid pUDR585. For *SpCas9*-gRNAs expressed by T7RNAP, T7-edged plasmid backbones were PCR amplified using primers 14274-15287 (*S.T7p/sgRNA-T7t*) or 14275-15287 (*L.T7p/sgRNA-T7t*), generating a dsDNA fragment that additionally contains a partial sequence of the gRNA scaffold for *SpCas9*. Gibson assemblies of annealed oligos 15290-15291 to either the *S.T7p/sgRNA-T7t* or *S.T7p/sgRNA-T7t* PCR-generated backbones were performed to obtain plasmids pUDR579 and pUDR581, respectively.

The control array of gRNAs expressed by plasmid pUDR692 was ordered as synthetic gene from GeneArt (Thermo Fisher Scientific). *SNR52* promoter and gRNA design principles previously elucidated were used.<sup>5</sup> The synthetic gRNA array was flanked by *BsaI* sites and assembled by Golden Gate cloning into pGGKd018.

### Delivery methods of gRNA expression cassettes

Each gRNA expression cassette was transformed together with 1 µg of double-stranded deletion repair (Table S1) in exponentially growing *S. cerevisiae* cells ( $\sim 2 \times 10^7$  cells ml<sup>-1</sup>), accordingly to the LiAc transformation protocol.<sup>27</sup> Genome editing via *in vitro* assembly described in Table 3 was prepared by transforming 500 ng ( $\sim 150$  fmols) of each gRNA expression plasmid. For genome editing achieved via *in vivo* plasmid assembly, two linear PCR fragments were delivered with the transformation mix: i) 150 fmols of the specific gRNA cassette, systematically amplified from the respective *in vitro* constructed plasmid using primers 14584-14585; ii) 150 fmols of the linearized marked  $2\mu$  backbone with 60 bp homology to each gRNA cassette, obtained from the amplification of pUDE810 with primers 11571-12378. To evaluate genome editing via delivery of linear gRNA expression cassette, each amplified gRNA cassette (150 fmols) was transformed with either 500 ng of circular pGGKd018 plasmid or with equimolar amount of two PCR fragments for the split plasmid selection using pGGKd018. These amplicons, having homologies for *in vivo* recircularization of the plasmid, were obtained by PCR amplification with primers 6815-9340 and primers 2398-12097.

All transformations were plated on selective YPD medium supplemented with G418. Efficiency of *ADE2* deletion is measured as number of red colonies on total colony forming unit (CFU). For editing of other sites, diagnostic PCR was performed on a number of selected colonies using primer listed in Table S1.

### Preparation of gDNAs and genome editing via gEL DNA

Sequences of deletion repair fragments and gDNAs are listed as forward and reverse oligonucleotides in Table S1. Site XI-3 is located at the previously characterized integration locus

on chromosome XI<sup>28</sup>, while XVI-1 corresponds to the intergenic region between *CUP9* and *TRE1* on chromosome XVI. The spacer for the non-targeting (nt) gDNA was designed by scrambling the *ADE2-3s* spacer sequence. Each forward and reverse oligo were mixed in equimolar amount, heated for 5 minutes at 95°C and cooled down to room temperature. As only exception, *SpCas9*-mediated editing using gDNA with long T7 promoter was obtained by PCR amplification of two overlapping primers, the gRNA-specific forward for *ADE2.y* (16745) and the universal reverse carrying the *SpCas9*-gRNA scaffold (16746). Concentrations of each double-stranded annealed oligos were measured for all pre-annealed oligos or the non-purified PCR-derived gDNA. 1 µg of each deletion repair and 4 µg of respective gDNA were mixed to 500 ng of split pGGKd18 plasmid for selection purposes and transformed into competent T7RNAP-expressing yeast cells accordingly to standard procedure.<sup>27</sup> Transformants were selected on YPD plates supplemented with G418 if transforming T7RNAP genomically integrated strains (IMX1905, IMX2030, IMX2031, IMX2032), or with G418 and hygromycin B if transforming T7RNAP-overexpressing strains (IME459, IME475) or for selection of the dual *FnCas12a*-T7RNAP overexpression strain (IME641). Plasmid-base controls for multiplex via *FnCas12a* gRNA-arrays were performed accordingly to Swiat *et al.*<sup>5</sup> Diagnostic PCR of selected colonies was done using primers listed in Table S1.

### Growth rate measurement

Strains were cultivated in 96-well plates containing SMD medium or SMD-urea supplemented with hygromycin B (30°C, 250 rpm). Growth was monitored by measuring optical density at 660 nm at regular time intervals using the Growth Profiler 960 (Enzyscreen B.V., Heemstede, The Netherlands). Maximum specific growth rates ( $\mu_{max}$ ) were calculated using the equation 1:  $X=X_0 e^{\mu t}$  in which  $\mu$  indicates the exponential growth rate, from four independent biological cultures.

### Bioinformatic analysis

The short sequence of the T7 promoter was mapped to CEN.PK113-7D reference<sup>34</sup> by using Bowtie aligner (version 1.2.1.1)<sup>35</sup>, with "--all" for reporting all alignments per input query.

The RNA secondary structure was predicted with the RNAstructure Web Server (<https://rna.urmc.rochester.edu/RNAstructureWeb/>)<sup>36</sup>. Temperature was set to 30°C (303.15 K). Self-folding free energy are obtained via the same webtool.

## Results

### T7RNAP-expressing *S. cerevisiae* as a platform strain for Cas-mediated genome editing

For T7 RNA polymerase (T7RNAP)-based expression of gRNAs, the bacteriophage T7RNAP, previously functionally expressed in the yeast nucleus, was chosen.<sup>30</sup> Flanked by the strong and constitutive *TDH3* promoter and *TEF1* terminator, T7RNAP was integrated in the genome of a *S. cerevisiae* strain from the CEN.PK family that constitutively expressed both *SpCas9* and *FnCas12a* (strain IMX1752; Table 1). Sanger sequencing of the resulting strain IMX1905 revealed a missense mutation in the coding sequence of the T7RNAP as compared to the canonical sequence (<https://www.uniprot.org/uniprot/P00573>), which resulted in the replacement of a lysine by an arginine at the amino acid 276 of the polymerase (corresponding to amino acid 286 when considering the NLS) (Fig. S1). As the strain characterized by Dower and Rosbash<sup>30</sup> contained the same amino acid substitution and was proven to be functional in yeast, we decided to keep this variant (from now on referred to as T7RNAP<sup>K276R</sup>) to test the gEL DNA approach.

Physiological characterization revealed that IMX1905, co-expressing T7RNAP<sup>K276R</sup>, *SpCas9* and *FnCas12a*, grew as fast as the prototrophic control strain CEN.PK113-7D in chemically defined medium supplemented with glucose as sole carbon source (specific growth rate of  $0.42 \pm 0.01 \text{ h}^{-1}$  for IMX1905 and  $0.44 \pm 0.01 \text{ h}^{-1}$  for CEN.PK113-7D) (Fig. 3). Expression of T7RNAP is therefore not toxic for *S. cerevisiae*.

### T7RNAP enables gRNA expression from linear and circular DNA and promotes *SpCas9*- and *FnCas12a*-mediated DNA editing in *S. cerevisiae*

The activity of the T7RNAP<sup>K276R</sup> in *S. cerevisiae* was evaluated by measuring the DNA editing efficiency of *SpCas9* and *FnCas12a* guided by gRNAs expressed from T7 promoter. Two different T7 promoter lengths were tested, the minimal T7 promoter of 17 bp (TAATACGACTCACTATA; referred to as S.T7p), and an extended T7 promoter sequence of 27 bp (GCCGGGAATTTAATACGACTCACTATA; referred to as L.T7p) known to improve the stability of the T7RNAP-promoter complex *in vitro*.<sup>37</sup> An in-depth alignment search showed that the S.T7p sequence does not occur in the *S. cerevisiae* genome, making unwanted transcription from the host genome highly unlikely. T7RNAP<sup>K276R</sup>-driven gRNA expression was compared with gRNA expression from the RNAPolIII-dependent *SNR52* promoter, largely adopted by the yeast community for CRISPR-Cas editing.<sup>1,5</sup> Downstream all three promoters, at the initially transcribed region (ITS), a guanine triplet was added to increase the T7RNAP transcriptional activity.<sup>38</sup> As previously reported for *SpCas9*<sup>19</sup>, the addition of this guanine triplet strongly improved T7RNAP-mediated expression for *FnCas12a*-based DNA editing (Fig. S2). Disruption of *ADE2*, leading to a red colony phenotype, was used to assess editing efficiency<sup>39</sup> in strain IMX1905 (Table 1). Spacers previously shown to guide *SpCas9* and *FnCas12a* to *ADE2* with high efficiency were chosen.<sup>1,5</sup> *SpCas9* and *FnCas12a* have different requirements for functionality, which results to different

compositions and size of the DNA cassette encoding the gRNA (from now on called gRNA cassette) (Table 3). The *ADE2.y* gRNA for *SpCas9* was used in its standard chimeric form including the trans-acting RNA (tracrRNA).<sup>1</sup> The *ADE2-3* gRNA for *FnCas12a* was reduced to the minimal 19 nt-long spacer enclosed by the matured direct repeats (DR), as recently described.<sup>40</sup> Thanks to *FnCas12a* minimal requirements for DNA targeting and editing (no tracrRNA, small DR and spacer), the gRNA cassettes for *FnCas12a* were substantially smaller than those for *SpCas9* (Table 3).

The most popular method for gRNA delivery is via *in vitro* assembly of the gRNA expression cassette on a plasmid, and transformation of this circular plasmid to yeast. As expected, expression of the gRNA cassette from *SNR52p* using this delivery method led to high efficiency in editing of the *ADE2* gene in all colonies tested with both *SpCas9* and *FnCas12a* (Table 3A). Conversely, T7RNAP<sup>K276R</sup>-based gRNA expression resulted in extremely low editing efficiency with *FnCas12a* (4.6% ± 0.2% for the short and 8.2% ± 3.2% for the long T7 promoter) and null or negligible editing with *SpCas9* (Table 3A). Next to delivering a ready-made gRNA plasmid, two parts, one carrying the gRNA and the other the selection marker, were transformed into yeast. These two parts were flanked by 60 bp homologous sequences to enable *in vivo* circularization upon transformation. This delivery method enabled the transient availability of the gRNA cassette as linear DNA fragment. While reducing editing efficiency for *SNR52p*-based gRNA expression by ca. 10%, this method slightly increased *ADE2* editing by T7RNAP<sup>K276R</sup>-mediated expression of gRNAs for both *SpCas9* and *FnCas12a* (Table 3B). Editing by *SpCas9* remained extremely low (around 1%), while up to 20% of the colonies displayed the disruption of *ADE2* by *FnCas12a* (Table 3B). Next, to test whether the gRNA could be solely expressed from a linear DNA molecule, the gRNA cassette was delivered as double-stranded DNA fragment. A plasmid carrying a selectable marker was transformed in parallel for selection purposes. With this delivery method, editing efficiency with RNAPolIII-mediated gRNA expression was dramatically reduced to ca. 10% with both *SpCas9* and *FnCas12a* (Table 3C). Editing efficiency for T7RNAP<sup>K276R</sup>-based gRNA expression was also reduced, but still detectable with ca 6% when using *FnCas12a*. It has been shown that the efficiency of *SpCas9*-mediated DNA editing can be increased by supplying a split plasmid during transformation, presumably by offering a selective advantage to cells that are proficient in homology directed repair.<sup>9</sup> Accordingly, a two-fold increase in *ADE2* editing efficiency was measured with both *SpCas9* and *FnCas12a* when the gRNAs were transcribed by RNAPolIII (Table 3C and D). However, using a circular or a split plasmid did not affect DNA editing for T7RNAP<sup>K276R</sup>-expressed gRNAs (Table 3C and D). The split marker approach combined with linear DNA delivery of the gRNA described in Table 3D was nonetheless kept for all the following experiments.

Altogether, these data demonstrate that gRNAs can be expressed from circular and linear DNA using the T7RNA<sup>K276R</sup> polymerase in *S. cerevisiae*. Additionally, *FnCas12a* leads to higher DNA

editing efficiency than *SpCas9* when guided by T7RNAP<sup>K276R</sup>-expressed gRNAs. In all experiments, the long T7 promoter consistently led to two- to three-fold higher editing efficiencies than the short T7 promoter (Table 3A and B), as possible consequence of the higher T7RNAP-promoter complex stability.<sup>37</sup> While delivery of gRNAs in the form of short linear DNA fragments enabled DNA editing, the observed editing efficiencies were low and required further optimization to turn the gEL DNA approach into an attractive and competitive DNA editing technique.

### Improving the efficiency of the T7RNAP<sup>K276R</sup>-based gEL DNA technique by optimizing the gDNA design

Aiming for cloning-free genome editing, the gEL DNA technique relies on the simple utilization of customized double-stranded DNA oligos (referred to as gDNAs) for the *in vivo* T7RNAP<sup>K276R</sup>-mediated expression of gRNAs. To reduce synthesis costs and increase compatibility with high-throughput strain construction, the size of the gDNA should be as small as possible and should not exceed 120 nt, the standard size limit of commercial, custom-made oligomers. In this respect, *FnCas12a* presents a clear advantage as its gRNAs consists of a smaller structural part (DR) than the one required for DNA targeting by *SpCas9* (gRNA scaffold). Consequently, the small size of *FnCas12a* gRNAs gives more flexibility in gDNA design regarding length of T7 transcriptional elements and presence of terminal DR or T7 terminator. Conversely, a minimal gDNA configuration for *SpCas9*-mediated editing containing the S.T7p and the chimeric gRNA is 119-nt long (Fig. 4), which does not leave room for additional, potentially useful parts such as a longer T7 promoter or a T7 terminator. As previously, a triplet of guanine was appended to the T7 promoter for all tested gDNA.

For *SpCas9*, two gDNA configurations were tested, one with the short and one with the long T7 promoter, followed by the *ADE2.y* spacer and the gRNA scaffold (Fig. 4A). As compared to the design presented in Table 3, no T7 terminator was added at the end of the gDNA. While the pre-annealed S.T7p gDNA can be directly transformed into IMX1905, the longer L.T7p gDNA (129 bp) had to be obtained by a preliminary PCR reaction using two primers with overlapping homologies (see Material and Methods section). Both gEL DNA configurations did enable *SpCas9*-mediated DNA editing, marginal for the S.T7p (2.6% editing efficiency, Fig. 4A-i) but substantial for the L.T7p (21% editing efficiency, Fig. 4A-ii).

Six different gDNA configurations for the *ADE2-3* target were tested for *FnCas12a*-mediated editing, differing in the size of T7 promoter and terminator as well as in the addition of a terminal DR and a T7 terminator (Fig. 4B). After simple pre-annealing of two complementary oligos *in vitro*, each gDNA was directly transformed into strain IMX1905. These data revealed that the terminal DR is important for efficient editing of *ADE2* irrespective to the presence of the T7 terminator, and that the presence of a T7 terminator is not required (Fig. 4B). These results also further confirmed that the long version of the T7 promoter markedly increased DNA editing efficiency (Fig. 4B, i-ii). This design optimization enabled to increase the DNA editing efficiency to 60%,



relying on the very simple transformation of yeast with an 87 nt-long oligonucleotide. This simple and efficient design, represented in Fig. 4B-ii, was implemented for the rest of the work with *FnCas12a*.

The editing efficiencies shown in Fig. 4 were substantially higher for both *SpCas9* and *FnCas12a* than those reported in Table 3D, in which a similar approach with linear gDNA delivery together with a split plasmid was also used. This increased efficiency most probably resulted from the higher amount of gDNA supplied to the transformation mix used for the experiments presented in Fig. 4 (300 to 400-fold higher). The increased editing efficiency combined with the higher abundance of gDNA suggests that a greater supply of the gDNA to the cell might be a key element for genome editing using gEL DNA.

### Improving the efficiency of the gEL DNA technique by optimizing sequence and expression levels of the T7RNAP

To further explore whether gDNA, and consequently gRNA availability might be limiting editing efficiency, gDNA transcription efficiency by the T7RNAP was explored. To this end, three additional T7RNAP variants were tested. All three variants were constructed from IMX1905, by inserting point mutations in the T7RNAP<sup>K276R</sup> gene. In the first variant the K276R mutation was reverted into the wild-type T7RNAP (*wt*T7RNAP, strain IMX2031). The second variant carried the P266L mutation, known to reduce abortive transcription *in vitro*<sup>41</sup> (T7RNAP<sup>P266L</sup>, strain IMX2032) and the third variant carried the two mutations (T7RNAP<sup>P266L, R276K</sup>, strain IMX2030). When tested with *FnCas12a*, all four variants enabled DNA editing with a significantly higher efficiency for T7RNAP<sup>P266L</sup> (Fig. 5), while T7RNAP<sup>K276R</sup> and T7RNAP<sup>P266L, R276K</sup> showed the lowest DNA editing efficiency (Fig. 5), suggesting that the K276R substitution is deleterious for T7RNAP transcription efficiency.

To further enhance gDNA transcription efficiency, the expression level of the T7RNAP was increased. The strains IME459 and IME475 were constructed by transformation with episomal plasmids harbouring the T7RNAP<sup>R276K</sup> and the T7RNAP<sup>P266L</sup> variants, respectively. While expression of T7RNAP from a single, integrated gene copy did not affect growth of *S. cerevisiae* (Fig. 3), expression from episomal vectors significantly reduced the growth rate when compared to a control strain carrying an empty episomal vector ( $0.29 \pm 0.00 \text{ h}^{-1}$  for IME459,  $0.26 \pm 0.01 \text{ h}^{-1}$  for IME475 and  $0.31 \pm 0.01 \text{ h}^{-1}$  for the control strain IME460, Fig. 3; Table 1). Overexpressing of either T7RNAP strongly increased the DNA editing efficiency by *FnCas12a*, approaching 100% when using T7RNAP<sup>P266L</sup> (Fig. 5). Overexpression of T7RNAP<sup>P266L</sup> also increased DNA editing efficiency by *SpCas9*, as compared to a single copy of T7RNAP<sup>K276R</sup>, but to a lesser extent (increase by 10%, Fig. 5). The gEL DNA approach remained much more efficient with *FnCas12a* than with *SpCas9* (maximum efficiencies of 96% and 29%, respectively, Fig. 5). Finally, to test whether the efficiency of gEL DNA was sensitive to location and sequence of the edited site, using these optimized conditions, three new sites were selected in non-coding regions and were tested for

*FnCas12a*-mediated targeting with the T7RNAP<sup>P266L</sup>-overexpression strain (IME475). The high efficiency of single gEL DNA editing was confirmed with efficiency between 90 and 100% for these three loci (XI-3<sup>28</sup>, XVI-1 and *YPRC*  $\tau$ 3 loci, Fig. S4).

Altogether these results revealed that the expression levels of the T7RNAP, and therefore most likely gRNA availability, play a key role for successful DNA editing by *FnCas12a* in the gEL DNA system.

### Assessment on the components required for efficient DNA editing using gEL DNA

In the approach described above, gEL DNA requires five components, the T7RNAP and *FnCas12a* already present in the transformed strain, and the gDNA cassette, repair DNA and split plasmid carrying the selection marker, delivered as linear fragments during transformation. Control experiments in which these components were systematically omitted confirmed that all five components are required for efficient DNA editing using the gEL DNA method (Fig. 6; Fig. S5). Editing was completely abolished in the absence of targeting gDNA and of repair DNA, as well as if the targeting gDNA was replaced by a non-targeting variant, with or without repair DNA. The supply of the split plasmid is understandably not essential for DNA editing using the gEL DNA method, but is key for the selection of edited transformants, as its absence resulted in an abundance of colonies on the plates and very low editing efficiency (ca. 8%). It is however remarkable that, even in the absence of selection marker, correctly edited transformants could be found. It is interesting to note that DNA editing was observed in the absence of T7RNAP, albeit with extremely low efficiency (ca. 8%). This editing was however abolished when *FnCas12a* was also omitted. As the presence of targeting gDNA is necessary for DNA editing by *FnCas12a* (Fig. 6, no editing in the absence of targeting gDNA), this T7RNAP-independent editing might be explained by low-level transcription of the supplied gDNA by one of the native yeast polymerases or by guiding of *FnCas12a* by single-stranded gDNA present as contamination of the double-stranded gDNA stock, although both hypothesis seem unlikely. Overall, *FnCas12a*, T7RNAP, gDNA, repair DNA and selection plasmid are essential for maximal DNA editing efficiency by gEL DNA.

### gEL DNA enables *FnCas12a*-mediated multiplex genome editing in *S. cerevisiae*

To test for multiplex genome editing, four gRNAs targeting *CAN1*, *HIS4*, *PDR12* and *ADE2*, previously shown to lead to 100% DNA editing efficiency by *FnCas12a* when expressed from a RNAPolIII promoter, were selected (<sup>5</sup>, Fig. 7A). As done for the *ADE2-3* target used for singleplex gEL DNA, these additional gRNAs were shortened to a 19 bp-long spacer as compared to the previously described plasmid-based constructs.<sup>5</sup> Oligos carrying the gDNA design shown in Fig. 4B-ii were ordered for each gRNA (Table S1) and transformed in duplex or quadruplex to IME475 overexpressing the T7RNAP<sup>P266L</sup>. Duplex targeting of *ADE2* and *HIS4* revealed that a vast majority of tested clones were edited (14 out of 16) and that 63% of the clones carried a double deletion



(Fig. 7B). Out of the clones with single editing, none carried a single *HIS4* deletion, while duplex editing with *ADE2* was clearly a frequent event (Fig. S6). Quadruplex targeting resulted in a substantial fraction of clones without any editing (34%, Fig. 7C). The fraction of clones with a single editing event was very similar for duplex and quadruplex editing (25 and 30%, respectively). 23% and 13% of the clones carried double and triple editing, respectively and quadruplex editing was not observed (Fig. 7C). Remarkably, none of the tested clones displayed editing in *CAN1* (Fig. S7), suggesting that the *CAN1-4* gRNA failed to guide *FnCas12a* to the targeted site. This lack of targeting might be explained by the fact that the *CAN1-4* gRNA contained an additional guanine triplet and was six nucleotides shorter than the *CAN1-4* gRNA originally tested by Swiat and co-workers. To test this hypothesis, the *CAN1-4* gDNA (GGG at his 5' and a 19 bp-long spacer) was expressed from a plasmid with the *SNR52* promoter and tested for editing efficiency. Out of eight selected colonies, none resulted in a *CAN1* deletion (Fig. S8), a complete loss in editing efficiency that is likely due to the disruption of the gRNA stem-loop structure (Table S3). A new *CAN1* spacer with a predicted secondary structure displaying the gRNA stem-loop was therefore selected for *CAN1* targeting (*CAN1-3*<sup>5</sup>, Table S3). Expressed from a plasmid with the *SNR52* promoter, *CAN1-3* led to 100% *CAN1* editing with *FnCas12a* (Fig. S8). However, when tested for multiplexing using the gEL DNA, *CAN1-3* rarely led to editing of *CAN1* by *FnCas12a* (Fig. 7D). A single *CAN1* editing event was observed out of 30 clones tested (Fig. S9) and, remarkably, this event was concomitant with the editing of the three other targets, leading to a single clone with quadruple DNA editing (Fig. 7D). In the quadruplex editing experiments with *CAN1-4* and *CAN1-3*, the fraction of clones with single, double and triple DNA editing was comparable (roughly 30, 25 and 10% respectively, Fig. 7C and D).

Following the approach described by Swiat and co-workers, two crRNA arrays were tested for quadruplex genome editing. Both plasmids carried the *HIS4-4*, *ADE2-3* and *PDR12-3* gRNAs, but pUDE735 expressed *CAN1-4* (Fig. S7) while pUDR692 expressed *CAN1-3* (Fig. S9). As previously observed, the number of colonies obtained after transformation was extremely low (below ten colonies), as compared to the number of colonies obtained for quadruplex editing with the gEL DNA approach (over 150 colonies).

### Construction and validation of a portable gEL DNA toolkit

The orthogonality of the T7RNAP-based gEL DNA system has great potential for other organisms. To demonstrate transportability, all-in-one multicopy plasmids carrying both T7RNAP and *FnCas12a* were constructed (pUDE1083, pUDE1084 and pUDE1087, Table 2). Both proteins have been shown to reduce growth rate when expressed individually at high level from multicopy plasmids (this work for T7RNAP and<sup>5</sup> for *FnCas12a*), simultaneous high-level expression of these two proteins might therefore be detrimental for the yeast strains. The results above show that the efficiency of DNA editing by gEL is sensitive to T7RNAP abundance, it was therefore decided to keep the same promoter for T7RNAP expression (*TDH3p*) but to tune the expression of *FnCas12a* by using three constitutive promoters spanning a broad range of strengths, *REV1p* with

low expression (resulting in strain IME646), *PFK1p* with intermediate expression (strain IME640) and the strong *TEF1p* (strain IME641). As expected, co-expression of T7RNAP and *FnCas12a* decreased the specific growth rate as compared to strains expressing T7RNAP or *FnCas12a* alone and to the control strain (ca. 20% decrease, Fig. S10), however strains with different promoter strengths for *FnCas12a* expression displayed similar growth rates (specific growth rate of  $0.26 \pm 0.01 \text{ h}^{-1}$  for IME640,  $0.25 \pm 0.01 \text{ h}^{-1}$  for IME641 and  $0.25 \pm 0.01 \text{ h}^{-1}$  for IME646; Figure S10). In the absence of promoter-dependent phenotypic effect, the strain expressing *FnCas12a* under the control of the strongest, *TEF1p* promoter (IME641) was selected to test the DNA editing efficiency of the portable gEL DNA system (plasmid map at Fig. 7E). Singleplex editing of *ADE2* revealed similar efficiencies between the integrated and portable systems (above 95 %  $\pm$  1% of edited colonies, Fig. S11). However, the portable system proved to be substantially superior for duplex and quadruplex editing (Fig. 7F and Fig. S12 and S13) with 100% and 30% efficiency for duplex and quadruplex editing, respectively. Remarkably, the remaining 70% of the colonies transformed for quadruplex editing displayed triplex editing, with *CAN1* systematically unedited (Fig. 7F). The plasmid-based gEL DNA approach is therefore highly efficient for singleplex and multiplex editing. It does not require a priori modification of target strain and is therefore a promising tool to be used in other yeasts, or even other organisms upon construction of compatible T7RNAP and *FnCas12a*-expressing plasmids.

## Discussion

The future of the CRISPR-Cas-based genome editing heads towards the development of fast and low- cost methodologies for strain construction. The gEL DNA approach presented in this study expands the CRISPR-Cas genome editing toolbox of *S. cerevisiae* with an entirely cloning-free and very efficient strategy for single or double genetic modification in *S. cerevisiae*. By simply transforming pre-annealed 87-long, complementary DNA oligonucleotides into competent yeast cells, cost and time of strain construction can be reduced to their bare minimum. Any chosen gRNA cassette can be delivered independently or in combination with other gRNA cassettes, making this technique very versatile and highly suitable for high-throughput, combinatorial strain construction. Akin to other CRISPR-based techniques for genome engineering increasing the number of simultaneously targeted sites strongly affects the efficiency of multiplexed gEL DNA or the viability of cells in terms of CFU on transformation plate (Table S2, Fig. 7).<sup>5,7</sup> The results obtained in this study suggest that this efficiency can be further enhanced. For instance, increasing T7RNAP and gDNA abundance substantially increased singleplex gene editing (Fig. 4, Fig. 5), suggesting that gRNA abundance might be a key factor for efficient DNA editing. Measurement of gRNA abundance should be performed to confirm this hypothesis, however, measurement of these extremely short, transiently expressed RNAs during transformation is technically extremely challenging. While the toxicity of plasmid-borne T7RNAP expression showed that its abundance cannot be further increased in *S. cerevisiae*, the efficiency of the gEL DNA could be further enhanced by T7RNAP protein engineering or by expression of DNA-dependent RNAP variants from other bacteriophages (*i.e.* T3, SP6 or K11) that are able to transcribe from short promoters and from linear DNA templates.<sup>42-44</sup> Another aspect to consider is the stability of the gDNA. While other methods deliver gRNA in the form of plasmids that are very stable *in vivo*, the linear nature of the gDNA make it prone to degradation by native exonucleases. Further studies should explore the stability of gDNA and gRNA during transformation and test whether chemical stabilization of the linear gDNA (by phosphorotioate derivatives or 2'-ribose modification for instance <sup>45,46</sup>) enhances gRNA availability and thereby DNA editing. There are therefore several promising avenues to further improve multiplex DNA editing with the gEL DNA approach.

Out of the eight gRNAs tested in this study, one failed to guide *FnCas12a* for gene editing. Remarkably, for this guide (*CAN1-4*) the folding prediction suggested the whole disruption of the direct repeat as a consequence of the 5'-addition of the guanine triplet, while the other seven guides displayed typical gRNA secondary structures with the required stem-loop structure (Fig. 7 and Table S3).<sup>47</sup> In agreement with these observations, a recent study about the *FnCas12a*-gRNA functionality suggests that the disruption of the direct repeat pseudoknot structure by pairing to the spacer sequence might lead to loss of gRNA targeting ability.<sup>40</sup> Additionally, inhibition of the gRNA processing and consequently of *FnCas12a* activity seems to be due to the positional effect

of a stable secondary structure flanking the direct repeat.<sup>48</sup> It has been recently advised that the terminator should be spaced-out by a 24 nt-long spacer to avoid steric effects with the pseudoknot formation and thereby allow correct gRNA folding.<sup>40</sup> Our findings support these theories, since a gRNA flanked by the short, 30-nt T7 terminator sequence that lacks the stem-loop structure has a 1.8-fold higher *ADE2* editing efficiency than a gRNA with the longer, 47-nt T7 terminator (Fig. 4B, iv-v). Prediction of the gRNA structure is therefore essential to optimize *FnCas12a*-based DNA editing with the gEL approach.

Despite efforts to improve editing with both *SpCas9* and *FnCas12a*, the latter proved to be more efficient for DNA editing with the gEL DNA method. The causes for *SpCas9* lower efficiency remain to be elucidated, but the observation that increasing T7RNAP abundance hardly affects DNA editing by *SpCas9* (increased by 1.4%; Fig. 5) suggests that gRNA abundance is not the factor impairing *SpCas9* activity. While the length of the gDNA might be another obstacle for *SpCas9* implementation with the gEL DNA approach, it could be overcome by expressing the tracrRNA separately from the gRNA.<sup>3</sup>

In conclusion, the gEL DNA methodology is not only an extremely valuable tool for genome editing in *S. cerevisiae*, but has a yet greater potential thanks to its portability to other organisms. Expression of gRNAs using the host machinery or *in vivo* burden of gRNA-expression plasmids can present serious obstacles for CRISPR/Cas9 based editing.<sup>2,49-52</sup> By introducing a T7RNAP and gDNA oligos, the gEL DNA approach dissociates gRNA production from the host polymerase and from plasmid templates, thereby entirely removing these obstacles.

## Supplementary data

Supplementary Data are available at online.

## Acknowledgment

We thank Melanie Wijsman and Ewout Knibbe for constructing strains IMX1714 and IMX1752, respectively, Sofia Dashko for cloning plasmid pGGKd034, and Marcel van den Broek for the sequence alignment of the T7 promoter to the whole *S. cerevisiae* genome.

## Author Confirmation Statement

PR and NXB performed the experiments. PR, NXB, JMD and PDL designed the experiments, analysed the results and wrote the manuscript. All co-authors have reviewed and approved of the manuscript prior to submission. The manuscript has been submitted solely to this journal and is not published, in press, or submitted elsewhere. An earlier draft of this manuscript was posted at bioRxiv (doi: <https://doi.org/10.1101/2020.05.22.110494>)

## Author Disclosure Statement:

No competing financial interests exist.

## Funding

This research received funding from the Netherland Organization of Scientific Research (NWO).

## Tables

Table 1 – *Saccharomyces cerevisiae* strains used in this study

Strain	Relevant genotype	Origin
CEN.PK113-7D	MATa MAL2-8c SUC2	20
IMX1714	MATa MAL2-8c SUC2 <i>sga1Δ::SpCas9-natNT2</i>	This study
IMX1752	MATa MAL2-8c SUC2 <i>sga1Δ::SpCas9-natNT2, X-2(*):FnCas12a</i>	This study
IMX1905	MATa MAL2-8c SUC2 <i>sga1Δ::SpCas9-natNT2, X-2(*):FnCas12a</i> <i>YPRCt3Δ::T7RNAP<sup>K276R</sup></i>	This study
IMX2030	MATa MAL2-8c SUC2 <i>sga1Δ::SpCas9-natNT2, X-2(*):FnCas12a</i> <i>YPRCt3Δ::T7RNAP<sup>P266L, K276R</sup></i>	This study
IMX2031	MATa MAL2-8c SUC2 <i>sga1Δ::SpCas9-natNT2, X-2(*):FnCas12a</i> <i>YPRCt3Δ::T7RNAP</i>	This study
IMX2032	MATa MAL2-8c SUC2 <i>sga1Δ::SpCas9-natNT2, X-2(*):FnCas12a</i> <i>YPRCt3Δ::T7RNAP<sup>P266L</sup></i>	This study
IME459	MATa MAL2-8c SUC2 <i>sga1Δ::SpCas9-natNT2, X-2(*):FnCas12a</i> pUDE866	This study
IME460	MATa MAL2-8c SUC2 <i>sga1Δ::SpCas9-natNT2, X-2(*):FnCas12a</i> pGGKd034	This study
IME475	MATa MAL2-8c SUC2 <i>sga1Δ::SpCas9-natNT2, X-2(*):FnCas12a</i> pUDE911	This study
IME638	MATa MAL2-8c SUC2 pUDE911	This study
IME639	MATa MAL2-8c SUC2 pUDE1082	This study
IME640	MATa MAL2-8c SUC2 pUDE1083	This study
IME641	MATa MAL2-8c SUC2 pUDE1084	This study
IME642	MATa MAL2-8c SUC2 pGGKd034	This study
IME645	MATa MAL2-8c SUC2 pUDE1086	This study
IME646	MATa MAL2-8c SUC2 pUDE1087	This study

(\*)Integration site at 194944-195980 of Chromosome X from Mikkelsen *et al.* <sup>28</sup>.

Table 2 – List of plasmids used in this study

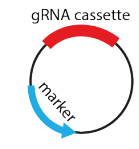

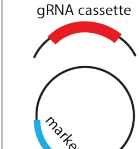
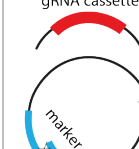


Plasmid	Genotype <sup>a</sup>	Reference
pUG-natNT2	amp <sup>R</sup> natMX	<sup>26</sup> , Addgene #110922
pYTK002	cam <sup>R</sup> ConLS	<sup>25</sup> , Addgene #65109
pYTK013	cam <sup>R</sup> <i>TEF1p</i>	<sup>25</sup> , Addgene #65120
pYTK027	cam <sup>R</sup> <i>REV1p</i>	<sup>25</sup> , Addgene #65134
pYTK036	cam <sup>R</sup> <i>SpCas9</i>	<sup>25</sup> , Addgene #65143
pYTK047	cam <sup>R</sup> GFPdo	<sup>25</sup> , Addgene #65154
pYTK051	cam <sup>R</sup> <i>ENO1t</i>	<sup>25</sup> , Addgene #65158
pYTK067	cam <sup>R</sup> ConR1	<sup>25</sup> , Addgene #65174
pYTK077	cam <sup>R</sup> KanMX	<sup>25</sup> , Addgene #65184
pYTK079	cam <sup>R</sup> HygR	<sup>25</sup> , Addgene #65186
pYTK082	cam <sup>R</sup> 2 μm	<sup>25</sup> , Addgene #65189
pYTK083	amp <sup>R</sup> <i>ColE1</i>	<sup>25</sup> , Addgene #65190
pYTK085	spec <sup>R</sup> <i>ColE1</i>	<sup>25</sup> , Addgene #65192
pUDE483	2 μm amp <sup>R</sup> <i>TEF1p::SpCas9::ENO1t</i>	This study
pUDC175	<i>CEN6/ARS4</i> amp <sup>R</sup> <i>TRP1 TEF1p::FnCas12a::CYC1t</i>	<sup>5</sup> , Addgene #103019
pUDR573	2 μm amp <sup>R</sup> amdSYM sgRNA-X-2	<sup>29</sup>
pRS315-nls-T7-RNAP	<i>CEN6/ARS4</i> amp <sup>R</sup> <i>LEU2 TDH3p::T7RNAP<sup>K276R</sup>::TDH3t</i>	<sup>30</sup> , Addgene #33152
pUD565	cam <sup>R</sup> GFPdo part entry vector	GeneArt
pGGKp172	cam <sup>R</sup> <i>T7RNAP<sup>K276R</sup></i>	This study
pGGKp035	cam <sup>R</sup> <i>TDH3p</i>	<sup>24</sup>
pGGKp039	cam <sup>R</sup> <i>TEF1t</i>	<sup>24</sup>
pGGKp100	cam <sup>R</sup> <i>PFK1p</i>	<sup>33</sup>
pGGKd034	2 μm amp <sup>R</sup> HygR GFPdo	This study
pUDE866	2 μm amp <sup>R</sup> HygR <i>TDH3p::T7RNAP<sup>K276R</sup>::TEF1t</i>	This study
pUDR477	2 μm spec <sup>R</sup> KanMX crYPRt3.3	This study
pGGKd018	2 μm spec <sup>R</sup> KanMX GFPdo	This study
pMEL13	2 μm amp <sup>R</sup> KanMX sgRNA-CAN1.Y	<sup>4</sup> , Euroscarf P30782
pUDE810	2 μm spec <sup>R</sup> KanMX <i>SNR52p::GFPdo::SUP4t</i>	This study
pUDE759	2 μm spec <sup>R</sup> KanMX <i>SNR52p::crADE2-3s::SUP4t</i>	This study
pUDR482	2 μm spec <sup>R</sup> KanMX <i>SNR52p::G-crADE2-3s::SUP4t</i>	This study
pUDR483	2 μm spec <sup>R</sup> KanMX <i>SNR52p::GG-crADE2-3s::SUP4t</i>	This study
pUDR484	2 μm spec <sup>R</sup> KanMX <i>SNR52p::GGG-crADE2-3s::SUP4t</i>	This study
pUDR485	2 μm spec <sup>R</sup> KanMX <i>S.T7p::crADE2-3s::T7t</i>	This study
pUDR486	2 μm spec <sup>R</sup> KanMX <i>S.T7p::G-crADE2-3s::T7t</i>	This study
pUDR487	2 μm spec <sup>R</sup> KanMX <i>S.T7p::GG-crADE2-3s::T7t</i>	This study
pUDR488	2 μm spec <sup>R</sup> KanMX <i>S.T7p::GGG-crADE2-3s::T7t</i>	This study
pUDR489	2 μm spec <sup>R</sup> KanMX <i>L.T7p::crADE2-3s::T7t</i>	This study
pUDR490	2 μm spec <sup>R</sup> KanMX <i>L.T7p::G-crADE2-3s::T7t</i>	This study
pUDR491	2 μm spec <sup>R</sup> KanMX <i>L.T7p::GG-crADE2-3s::T7t</i>	This study
pUDR492	2 μm spec <sup>R</sup> KanMX <i>L.T7p::GGG-crADE2-3s::T7t</i>	This study
pUDR585	2 μm spec <sup>R</sup> KanMX <i>SNR52p::GGG-sgRNA-ADE2.Y::SUP4t</i>	This study
pUDR579	2 μm spec <sup>R</sup> KanMX <i>S.T7p::GGG-sgRNA-ADE2.Y::T7t</i>	This study
pUDR581	2 μm spec <sup>R</sup> KanMX <i>L.T7p::GGG-sgRNA-ADE2.Y::T7t</i>	This study
pUDR506	2 μm amp <sup>R</sup> KanMX gRNA-T7RNAP	This study
pUDE911	2 μm amp <sup>R</sup> HygR <i>TDH3p::T7RNAP<sup>P266L</sup>::TEF1t</i>	This study
pUDE710	2 μm KanMX amp <sup>R</sup> <i>SNR52p::crADE2-3.crHIS4-4::SUP4t</i>	<sup>5</sup> , Addgene #103020

<b>pUDE735</b>	2 $\mu$ m KanMX amp <sup>R</sup> <i>SNR52p::crCAN1-4.crHIS4-4.crPDR12-3.crADE2-3::SUP4t</i>	<sup>5</sup> , Addgene #103024
<b>pUDR692</b>	2 $\mu$ m KanMX amp <sup>R</sup> <i>SNR52p::crCAN1-3.crHIS4-4.crPDR12-3.crADE2-3::SUP4t</i>	This study
<b>pUDR715</b>	2 $\mu$ m spec <sup>R</sup> KanMX <i>SNR52p::GGG-crHIS4-4s::SUP4t</i>	This study
<b>pUDR716</b>	2 $\mu$ m spec <sup>R</sup> KanMX <i>SNR52p::GGG-crPDR12-3s::SUP4t</i>	This study
<b>pUDR717</b>	2 $\mu$ m spec <sup>R</sup> KanMX <i>SNR52p::GGG-crCAN1-4s::SUP4t</i>	This study
<b>pUDR718</b>	2 $\mu$ m spec <sup>R</sup> KanMX <i>SNR52p::GGG-crCAN1-3s::SUP4t</i>	This study
<b>pUDE1082</b>	2 $\mu$ m amp <sup>R</sup> HygR <i>PFK1p::FnCas12a::CYC1t</i>	This study
<b>pUDE1083</b>	2 $\mu$ m amp <sup>R</sup> HygR <i>PFK1p::FnCas12a::CYC1t</i> <i>TDH3p::T7RNAP<sup>P266L</sup>::TEF1t</i>	This study
<b>pUDE1084</b>	2 $\mu$ m amp <sup>R</sup> HygR <i>TEF1p::FnCas12a::CYC1t</i> <i>TDH3p::T7RNAP<sup>P266L</sup>::TEF1t</i>	This study
<b>pUDE1086</b>	2 $\mu$ m amp <sup>R</sup> HygR <i>REV1p::FnCas12a::CYC1t</i>	This study
<b>pUDE1087</b>	2 $\mu$ m amp <sup>R</sup> HygR <i>REV1p::FnCas12a::CYC1t</i> <i>TDH3p::T7RNAP<sup>P266L</sup>::TEF1t</i>	This study
<p><sup>a</sup> ‘sgRNA’ denotes single-guide RNA used by Cas9, ‘cr’ refers to crRNA for <i>FnCas12a</i>. The presence of an ‘s’ following the crRNA indicates that a shorter spacer of 19 nt is used, otherwise the spacer size is 25 nt.</p>		



Table 3 – Comparing gRNA delivery methods

*SpCas9*- and *FnCas12a*-mediated DNA editing efficiency in IMX1905 (Table 1) transformed with different delivery methods for gRNA-expression cassette. A) *in vitro* pre-assembled plasmids; B) *in vivo* assembly after co-transformation of gRNA expression cassette and marker backbone with homology flanks; C) co-transformation of gRNA expression cassette with circular empty plasmid (pGGKd018); D) co-transformation of gRNA expression cassette with split empty plasmid (pGGKd018). The gRNA cassettes specific for *SpCas9* and *FnCas12a* editing are depicted at the left of the table (*p*, promoter; DR, direct repeat; *t*, terminator) and their respective length in bp is reported. These were compared for expression under the RNAPolIII-dependent SNR52*p* (pUDR585 for *SpCas9*, pUDR484 for *FnCas12a*), the T7RNAP-dependent 17bp-long S.T7*p* (pUDR579 for *SpCas9*, pUDR488 for *FnCas12a*) or the T7RNAP-dependent 27bp-long L.T7*p* (pUDR581 for *SpCas9*, pUDR492 for *FnCas12a*). Editing efficiency is expressed as percentage of red colonies (*ade2*<sup>-</sup>). Data represent the average and standard deviation of biological triplicates.

				<i>ade2</i> <sup>-</sup> frequency (%)				
				A. <i>in vitro</i> assembly	B. <i>in vivo</i> assembly	C. circular plasmid	D. split plasmid	
				gRNA cassette	gRNA cassette	gRNA cassette	gRNA cassette	
								
	<i>prom</i>	<i>term</i>	Size of gRNA cassette (bp)					
<b>gRNA cassette for <i>SpCas9</i></b>	SNR52	SUP4	401	100.0 ± 0.0	90.7 ± 1.7	11.4 ± 4.0	23.8 ± 6.6	
		S.T7	T7	166	0.0 ± 0.0	0.6 ± 0.4	–	–
	L.T7	T7	176	0.2 ± 0.2	1.2 ± 0.9	0.0 ± 0.0	0.0 ± 0.0	
<b>gRNA cassette for <i>FnCas12a</i></b>	SNR52	SUP4	359	100.0 ± 0.0	87.1 ± 4.5	12.3 ± 3.8	30.7 ± 5.2	
		S.T7	T7	124	4.6 ± 0.2	7.8 ± 3.8	–	–
	L.T7	T7	134	8.2 ± 3.2	20.1 ± 4.9	5.7 ± 1.9	6.7 ± 2.9	

## Figures

### Figure legends

**Figure 1: cloning-free approaches for CRISPR/Cas-aided DNA editing.** Overview of methodologies based on delivery of linear DNA templates for gRNAs expression in *S. cerevisiae*. *In vitro* sample preparations and *in vivo* events upon transformation are described. All gRNA expression cassettes include a RNAPolIII terminator. Number of PCR reactions are quoted. Features are depicted in the legend at the right-hand side of the figure.

**Figure 2: Schematic overview of the gEL DNA approach.** 1, *in silico* design and ordering of gDNA cassettes (87 bp) and repair DNA (120 bp) as oligos. 2, transformation with the double-stranded (ds) gDNA expression cassettes (2a), the ds repair DNA fragments (2b) and an empty, split plasmid carrying a marker of choice (2c). 3, expression of the gRNA by the T7RNAP. 4, targeted DNA editing by *FnCas12a*. 5, repair of the ds DNA break via homologous recombination using the repair DNA fragments.

**Figure 3: Physiological characterization of *S. cerevisiae* strains expressing T7RNAP.** Maximum specific growth rates ( $\mu_{max}$ ) of *S. cerevisiae* constitutively expressing T7RNAP<sup>K276R</sup>, *SpCas9* and *FnCas12a* (IMX1905) and its control strain (CENPK.113-7D), or *S. cerevisiae* strains overexpressing T7RNAP<sup>K276R</sup> (IME459) or T7RNAP<sup>P266L</sup> (IME475) and its control strain carrying a 2 $\mu$ m multi-copy empty vector (IME460). All strains were cultivated in 96-well plate containing chemically defined medium supplemented with glucose as sole carbon source (SMD for CENPK.113-7D or IMX1905; SMD-urea with hygromycin B for IME459, IME475 or IME460). The slower growth rate measured for strains with plasmids as compared to strains with genomic integration is explained by the difference in medium composition). Data points represent average and mean deviations of four biological replicates. \* $P < 0.025$ , \*\* $P < 0.001$ , Student's *t*-test was calculated compared to respective control strains CENPK.113-7D or IME460.

**Figure 4: Optimization of *SpCas9* and *FnCas12a* gDNA design.** Editing efficiency of *ADE2* in strain IMX1905 transformed with gDNAs for cloning-free, T7RNAP-driven expression of gRNA. A) gDNA configurations for *SpCas9*-mediated genome editing and respective editing efficiencies. B) gDNA configurations for *FnCas12a*-mediated genome editing and their respective editing efficiencies. The size of each gDNA is specified on the right of the respective graph bar. Editing efficiency is expressed as percentage of red colonies (*ade2*<sup>-</sup>) over the total number of colonies. Values represent the average and standard deviations of data obtained from three independent biological replicates.

**Figure 5: Comparison of *SpCas9* and *FnCas12a* editing efficiency with T7RNAP variants.** Efficiency of *ADE2* editing by *FnCas12a*- or *SpCas9*-mediated gEL DNA in T7RNAP mutant or overexpression strains: IMX1905 (K276R); IMX2031 (wild-type, *wt*); IMX2032 (P266L); IMX2030

(P266L\_K276R); IME459 (K276R overexpression,  $\nearrow$ K276R); IME475 (P266L overexpression,  $\nearrow$ P266L). For *FnCas12a*, transformed gDNA corresponds to annealed 15093-15094 oligos. For *SpCas9*, transformed gDNA was obtained by PCR-derived fragment using overlapping primers 16745-16746. Editing efficiency is expressed as percentage of red colonies (*ade2*<sup>-</sup>). Values represent the average and standard deviations of data obtained from independent biological duplicates. \**P* < 0.05, \*\**P* < 0.025, \*\*\**P* < 0.001, Student's *t*-test was calculated compared to respective control strain IMX1905 (K276R).

**Figure 6: CFU and ADE2 editing efficiencies with different combinations of the components of the gEL DNA system.** *S. cerevisiae* strains carrying *FnCas12a* and T7RNAP (IME475), *FnCas12a* alone (IMX1714) or control strain (CEN.PK-113.7D) were transformed with *ADE2* or non-targeting (nt) gDNAs, alternatively omitting repair DNA for *ADE2* deletion or split pGGKd018 plasmid for selection. Results of cell counts are presented as log CFU/mL. Editing efficiency is expressed as percentage of red colonies (*ade2*<sup>-</sup>), which were further verified by PCR (Fig. S5).

**Figure 7: Multiplex genome editing by *FnCas12a*-mediated using the gEL DNA approach.** (A) Targeted sites for deletion of *ADE2* (ADE2-3, green), *HIS4* (HIS4-4, orange), *PDR12* (PDR12-3, cyan) and *CAN1* (CAN1-4, pink; CAN1-3, violet) genes. (B) Percentage of IME475 (T7RNAP overexpression,  $\nearrow$ T7RNAP) transformants obtained from double gDNAs delivery: ADE2-3 and HIS4-4. (C) Fraction of selected colonies upon transformation of IME475 with four gDNAs: ADE2-3, HIS4-4, PDR12-3 and CAN1-4. (D) Fraction of selected colonies upon transformation of IME475 with four gDNAs: ADE2-3, HIS4-4, PDR12-3 and CAN1-3. (E) Plasmid map of the exportable gEL DNA plasmid pUDE1084. (F) Fraction of selected colonies upon transformation of IME641 (*FnCas12a* and T7RNAP overexpression,  $\nearrow$ *FnCas12a*  $\nearrow$ T7RNAP) with four gDNAs: ADE2-3, HIS4-4, PDR12-3 and CAN1-3. Number of verified clones is indicated between brackets and diagnostic PCRs are reported in Supplementary Figures (Fig. S6, S7, S9, S12, S13). Zero (0 $\Delta$ ), single (1 $\Delta$ ), double (2 $\Delta$ ), triple (3 $\Delta$ ) or quadruple (4 $\Delta$ ) deletion are indicated at the outside ends of each fraction. Type of obtained deletions are specified with the respective colour of the target. The number of tested colonies are also stated next to each depiction between bracket.

Figure 1

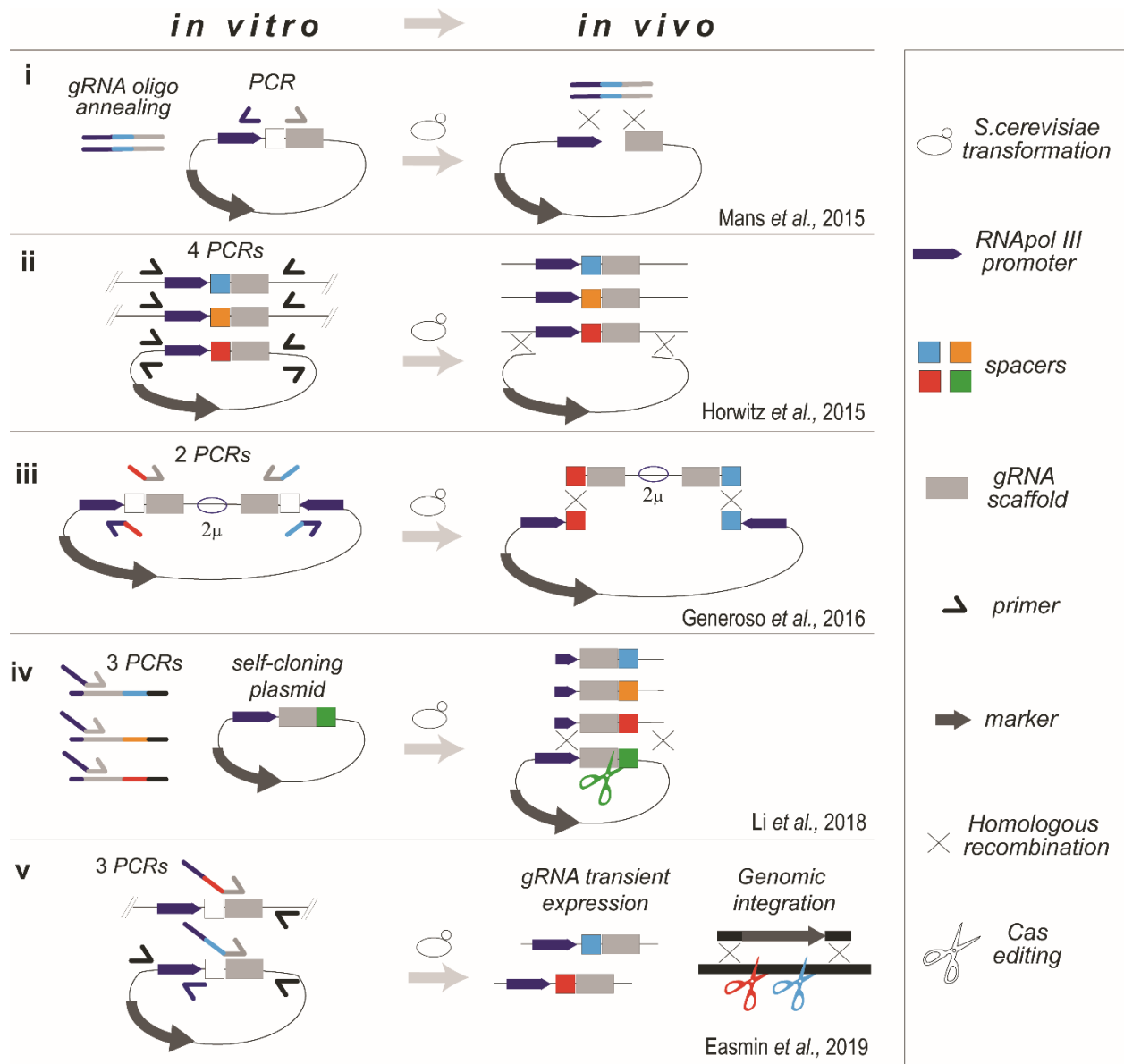


Figure 2

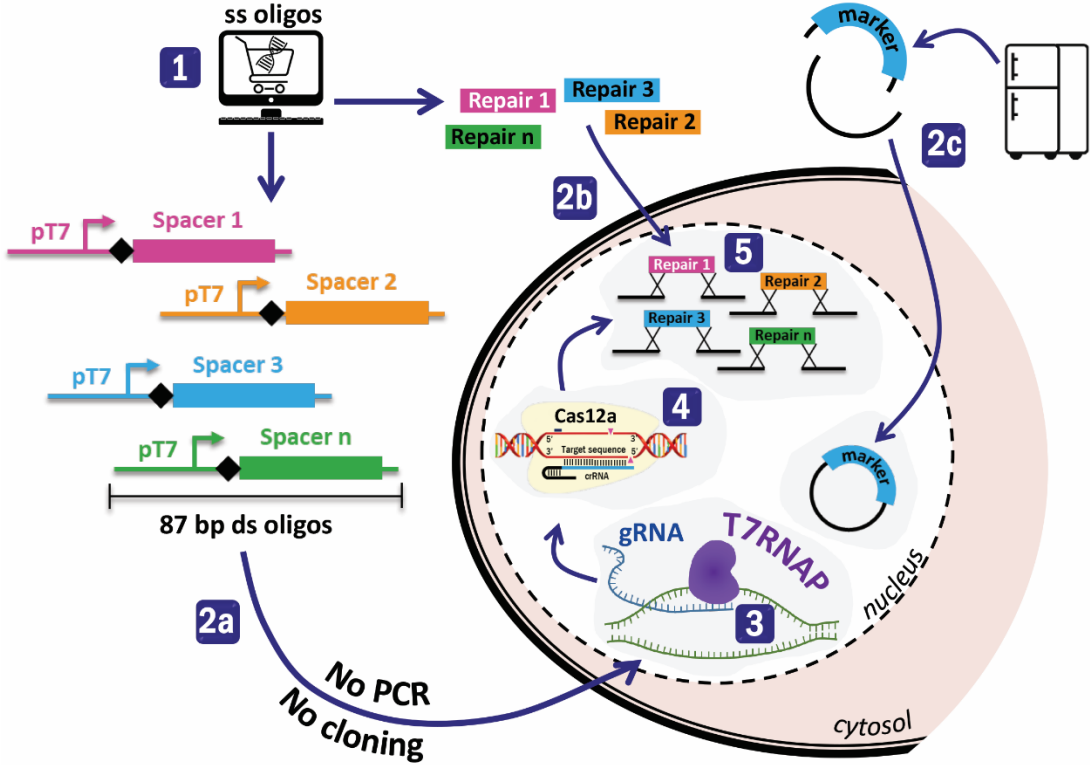


Figure 3

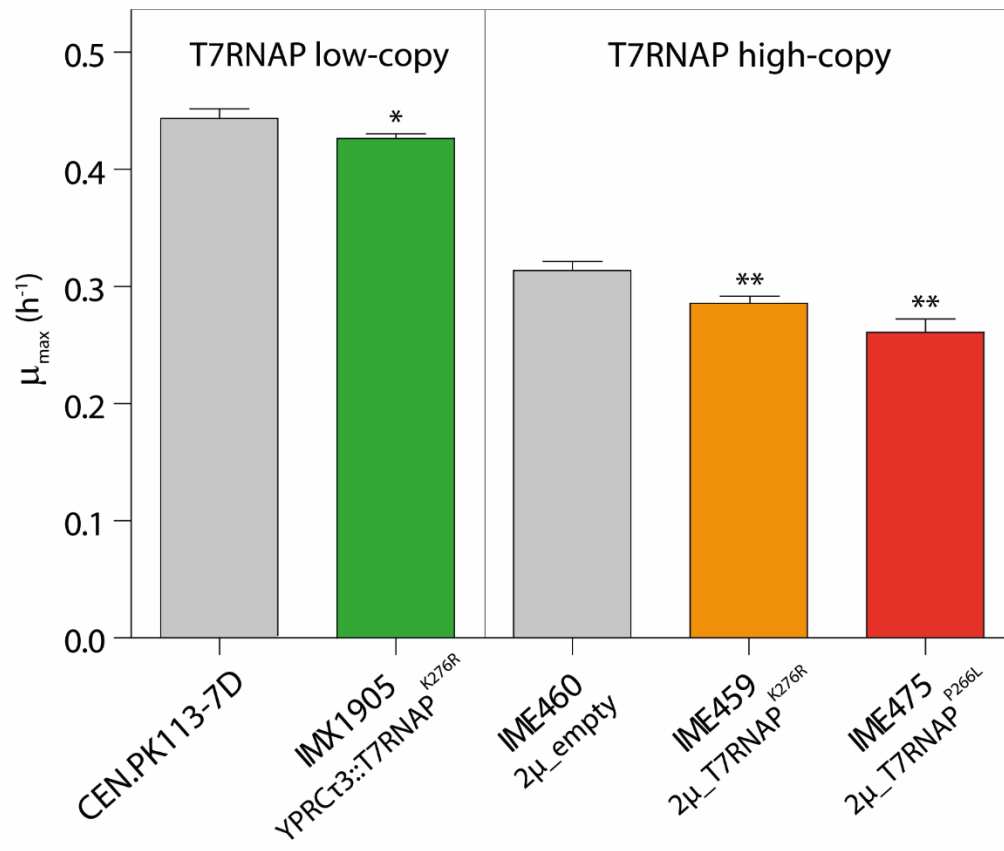


Figure 4

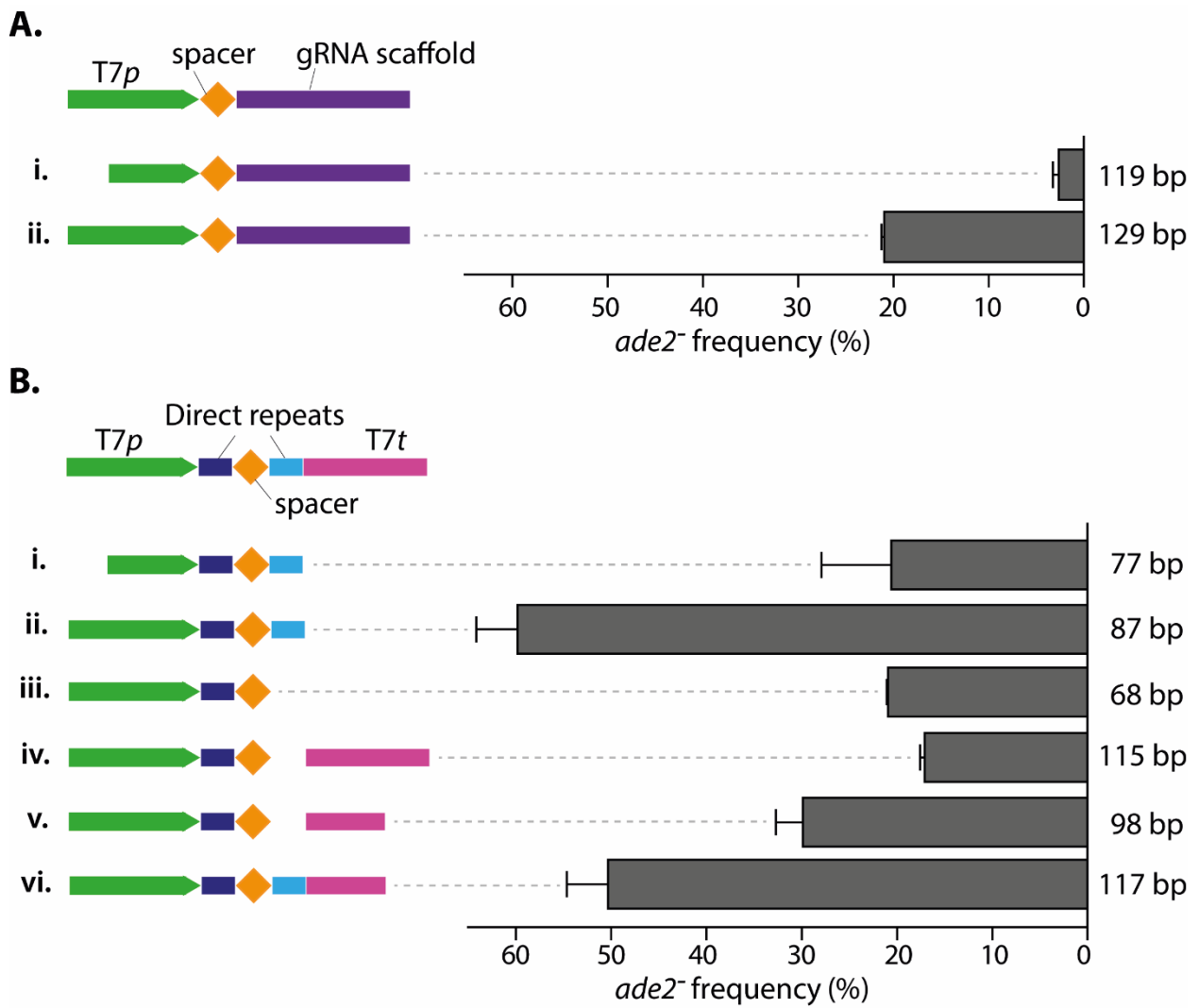


Figure 5

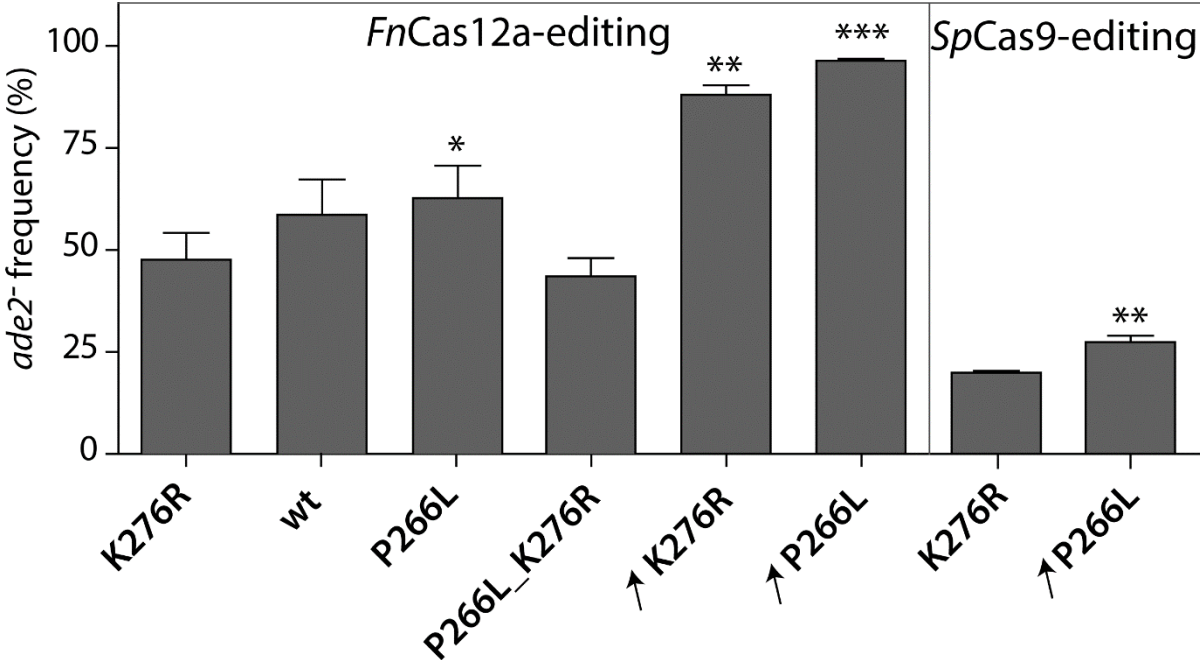




Figure 6

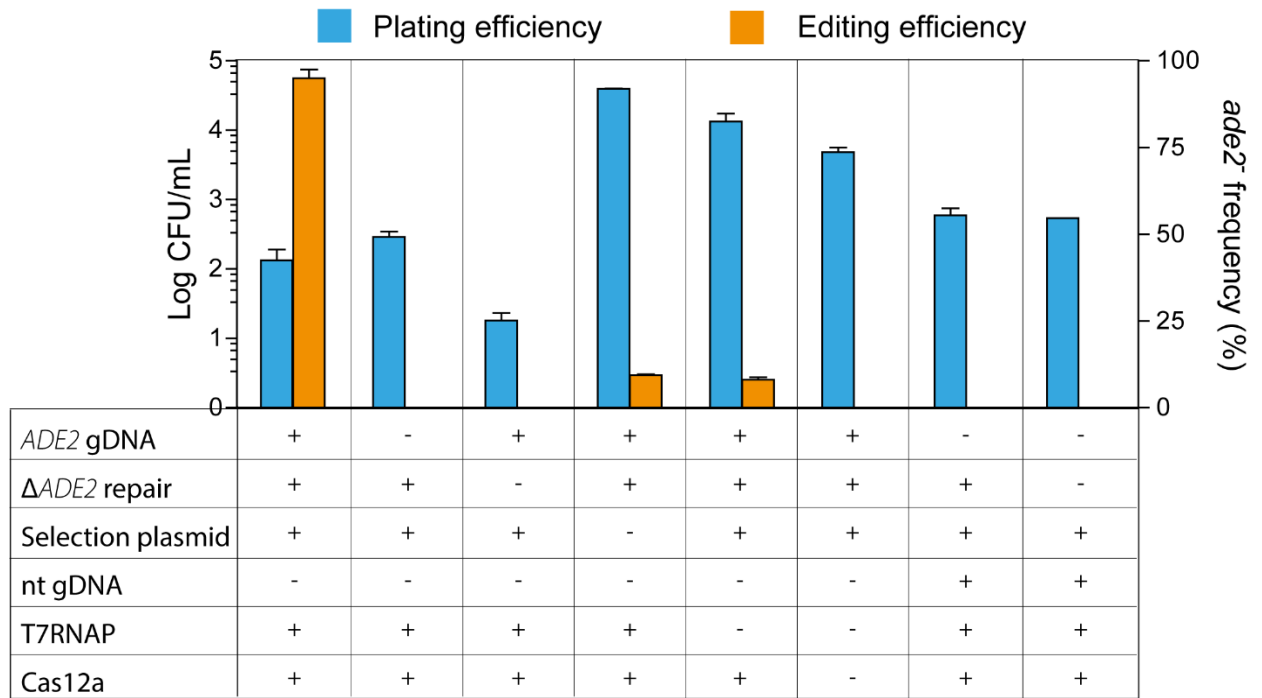
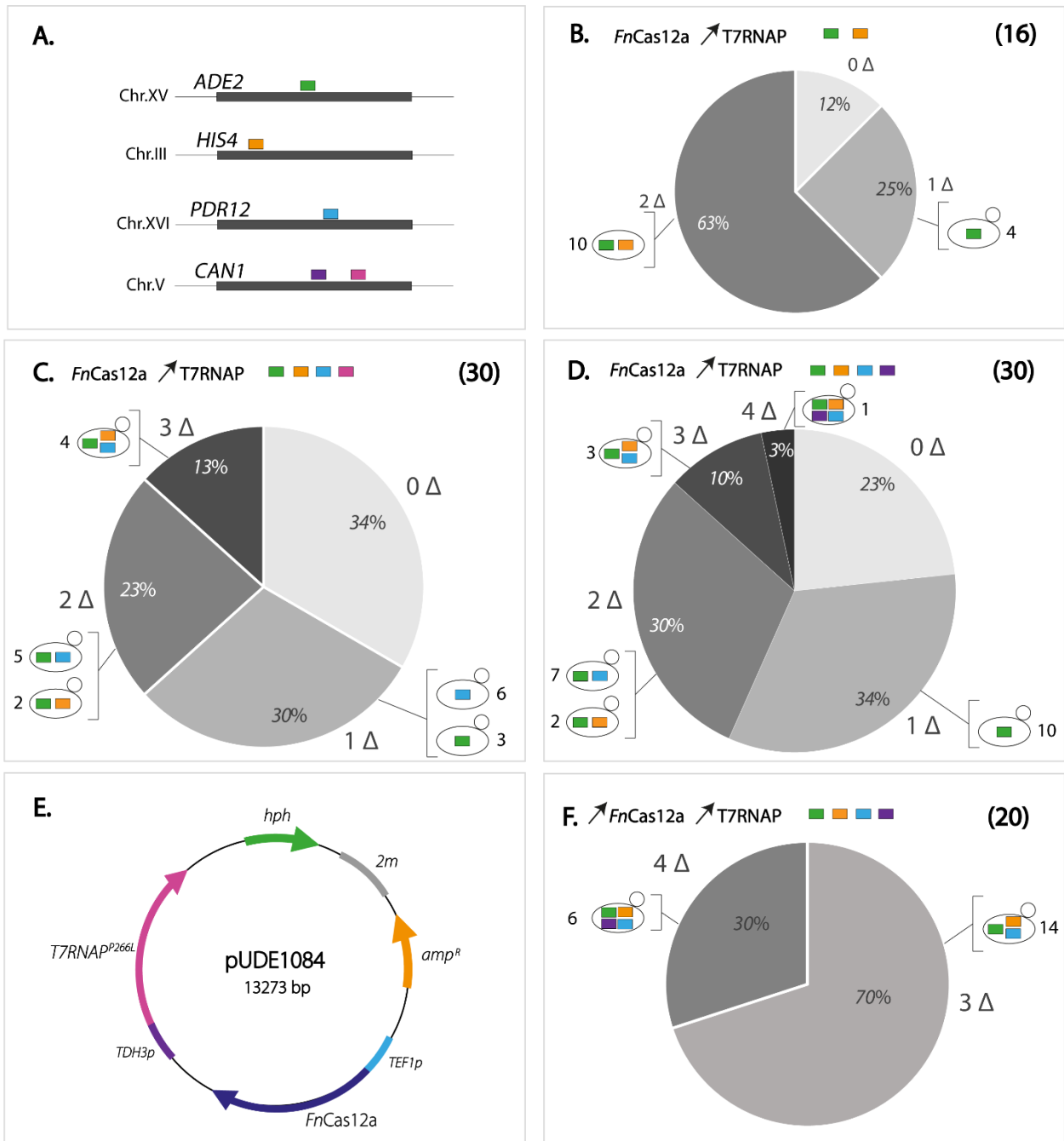


Figure 7



## References

1. DiCarlo JE, Norville JE, Mali P, et al. Genome engineering in *Saccharomyces cerevisiae* using CRISPR-Cas systems. *Nucleic Acids Res* 2013;41:4336-4343. doi: 10.1093/nar/gkt135.
2. Gao Y,Zhao Y. Self-processing of ribozyme-flanked RNAs into guide RNAs *in vitro* and *in vivo* for CRISPR-mediated genome editing. *J Integr Plant Biol* 2014;56:343-349. doi: 10.1111/jipb.12152.
3. Bao Z, Xiao H, Liang J, et al. Homology-integrated CRISPR-Cas (HI-CRISPR) system for one-step multigene disruption in *Saccharomyces cerevisiae*. *ACS Synth Biol* 2015;4:585-594. doi: 10.1021/sb500255k.
4. Mans R, van Rossum HM, Wijsman M, et al. CRISPR/Cas9: a molecular Swiss army knife for simultaneous introduction of multiple genetic modifications in *Saccharomyces cerevisiae*. *FEMS Yeast Res* 2015;15. doi: 10.1093/femsyr/fov004.
5. Swiat MA, Dashko S, den Ridder M, et al. FnCpf1: a novel and efficient genome editing tool for *Saccharomyces cerevisiae*. *Nucleic Acids Res* 2017;45:12585-12598. doi: 10.1093/nar/gkx1007.
6. Verwaal R, Buiting-Wiessenhaan N, Dalhuijsen S, et al. CRISPR/Cpf1 enables fast and simple genome editing of *Saccharomyces cerevisiae*. *Yeast* 2018;35:201-211. doi: 10.1002/yea.3278.
7. Adiego-Perez B, Randazzo P, Daran JM, et al. Multiplex genome editing of microorganisms using CRISPR-Cas. *FEMS Microbiol Lett* 2019;366. doi: 10.1093/femsle/fnz086.
8. Ryan OW, Skerker JM, Maurer MJ, et al. Selection of chromosomal DNA libraries using a multiplex CRISPR system. *eLife* 2014;3. doi: 10.7554/eLife.03703.
9. Horwitz AA, Walter JM, Schubert MG, et al. Efficient multiplexed integration of synergistic alleles and metabolic pathways in yeasts via CRISPR-Cas. *Cell Syst* 2015;1:88-96. doi: 10.1016/j.cels.2015.02.001.
10. Jakočiūnas T, Bonde I, Herrgård M, et al. Multiplex metabolic pathway engineering using CRISPR/Cas9 in *Saccharomyces cerevisiae*. *Metab Eng* 2015;28:213-222. doi: 10.1016/j.ymben.2015.01.008.
11. Walter JM, Chandran SS,Horwitz AA. CRISPR-Cas-Assisted Multiplexing (CAM): simple same-day multi-locus engineering in yeast. *J Cell Physiol* 2016;231:2563-2569. doi: 10.1002/jcp.25375.
12. Li Z-H, Wang F-Q,Wei D-Z. Self-cloning CRISPR/Cpf1 facilitated genome editing in *Saccharomyces cerevisiae*. *Bioresources and Bioprocessing* 2018;5:36. doi: 10.1186/s40643-018-0222-8.

13. Generoso WC, Gottardi M, Oreb M, et al. Simplified CRISPR-Cas genome editing for *Saccharomyces cerevisiae*. *J Microbiol Methods* 2016;127:203-205. doi: 10.1016/j.mimet.2016.06.020.
14. Ferreira R, Skrekas C, Nielsen J, et al. Multiplexed CRISPR/Cas9 genome editing and gene regulation using Csy4 in *Saccharomyces cerevisiae*. *ACS Synth Biol* 2018;7:10-15. doi: 10.1021/acssynbio.7b00259.
15. Li ZH, Liu M, Lyu XM, et al. CRISPR/Cpf1 facilitated large fragment deletion in *Saccharomyces cerevisiae*. *J Basic Microb* 2018;58:1100-1104. doi: 10.1002/jobm.201800195.
16. Zhang Y, Wang J, Wang Z, et al. A gRNA-tRNA array for CRISPR-Cas9 based rapid multiplexed genome editing in *Saccharomyces cerevisiae*. *Nat Commun* 2019;10:1053. doi: 10.1038/s41467-019-09005-3.
17. Ryan OW, Cate JH. Multiplex engineering of industrial yeast genomes using CRISPRm. *Methods Enzymol* 2014;546:473-489. doi: 10.1016/B978-0-12-801185-0.00023-4.
18. Easmin F, Hassan N, Sasano Y, et al. gRNA-transient expression system for simplified gRNA delivery in CRISPR/Cas9 genome editing. *J Biosci Bioeng* 2019. doi: 10.1016/j.jbiosc.2019.02.009.
19. Morse NJ, Wagner JM, Reed KB, et al. T7 Polymerase expression of guide RNAs *in vivo* allows exportable CRISPR-Cas9 editing in multiple yeast hosts. *ACS Synth Biol* 2018;7:1075-1084. doi: 10.1021/acssynbio.7b00461.
20. Entian KD, Kotter P. Yeast genetic strain and plasmid collections. *Method Microbiol* 2007;36:629-666. doi: 10.1016/S0580-9517(06)36025-4.
21. Verduyn C, Postma E, Scheffers WA, et al. Effect of benzoic acid on metabolic fluxes in yeasts: a continuous-culture study on the regulation of respiration and alcoholic fermentation. *Yeast* 1992;8:501-517. doi: 10.1002/yea.320080703.
22. Milne N, Luttk MAH, Cueto Rojas HF, et al. Functional expression of a heterologous nickel-dependent, ATP-independent urease in *Saccharomyces cerevisiae*. *Metab Eng* 2015;30:130-140. doi: 10.1016/j.ymben.2015.05.003.
23. Solis-Escalante D, Kuijpers NG, Bongaerts N, et al. amdSYM, a new dominant recyclable marker cassette for *Saccharomyces cerevisiae*. *FEMS Yeast Res* 2013;13:126-139. doi: 10.1111/1567-1364.12024.
24. Hassing EJ, de Groot PA, Marquenie VR, et al. Connecting central carbon and aromatic amino acid metabolisms to improve *de novo* 2-phenylethanol production in *Saccharomyces cerevisiae*. *Metab Eng* 2019;56:165-180. doi: 10.1016/j.ymben.2019.09.011.
25. Lee ME, DeLoache WC, Cervantes B, et al. A highly characterized yeast toolkit for modular, multipart assembly. *ACS Synth Biol* 2015;4:975-986. doi: 10.1021/sb500366v.

26. de Kok S, Nijkamp JF, Oud B, et al. Laboratory evolution of new lactate transporter genes in a *jen1Δ* mutant of *Saccharomyces cerevisiae* and their identification as *ADY2* alleles by whole-genome resequencing and transcriptome analysis. *FEMS Yeast Res* 2012;12:359-374. doi: 10.1111/j.1567-1364.2012.00787.x.
27. Gietz RD, Schiestl RH. High-efficiency yeast transformation using the LiAc/SS carrier DNA/PEG method. *Nat Protoc* 2007;2:31-34. doi: 10.1038/nprot.2007.13.
28. Mikkelsen MD, Buron LD, Salomonsen B, et al. Microbial production of indolylglucosinolate through engineering of a multi-gene pathway in a versatile yeast expression platform. *Metab Eng* 2012;14:104-111. doi: 10.1016/j.ymben.2012.01.006.
29. Baldi N, Dykstra JC, Luttk MAH, et al. Functional expression of a bacterial alpha-ketoglutarate dehydrogenase in the cytosol of *Saccharomyces cerevisiae*. *Metab Eng* 2019;56:190-197. doi: 10.1016/j.ymben.2019.10.001.
30. Dower K, Rosbash M. T7 RNA polymerase-directed transcripts are processed in yeast and link 39 end formation to mRNA nuclear export. *RNA* 2002;8:686-697. doi: 10.1017/s1355838202024068.
31. Flagfeldt D, Siewers V, Huang L, et al. Characterization of chromosomal integration sites for heterologous gene expression in *Saccharomyces cerevisiae*. *Yeast* 2009;26:545-551. doi: 10.1002/yea.1705.
32. Meijnen JP, Randazzo P, Foulquie-Moreno MR, et al. Polygenic analysis and targeted improvement of the complex trait of high acetic acid tolerance in the yeast *Saccharomyces cerevisiae*. *Biotechnol Biofuels* 2016;9:5. doi: 10.1186/s13068-015-0421-x.
33. Boonekamp FJ, Dashko S, van den Broek M, et al. The genetic makeup and expression of the glycolytic and fermentative pathways are highly conserved within the *Saccharomyces* genus. *Front Genet* 2018;9:504-504. doi: 10.3389/fgene.2018.00504.
34. Salazar AN, Gorter de Vries AR, van den Broek M, et al. Nanopore sequencing enables near-complete *de novo* assembly of *Saccharomyces cerevisiae* reference strain CEN.PK113-7D. *FEMS Yeast Res* 2017;17. doi: 10.1093/femsyr/fox074.
35. Langmead B, Trapnell C, Pop M, et al. Ultrafast and memory-efficient alignment of short DNA sequences to the human genome. *Genome Biol* 2009;10:R25. doi: 10.1186/gb-2009-10-3-r25.
36. Bellaousov S, Reuter JS, Seetin MG, et al. RNAstructure: Web servers for RNA secondary structure prediction and analysis. *Nucleic Acids Res* 2013;41:471-474. doi: 10.1093/nar/gkt290.
37. Tang GQ, Bandwar RP, Patel SS. Extended upstream A-T sequence increases T7 promoter strength. *J Biol Chem* 2005;280:40707-40713. doi: 10.1074/jbc.M508013200.

38. Imburgio D, Rong M, Ma K, et al. Studies of promoter recognition and start site selection by T7 RNA polymerase using a comprehensive collection of promoter variants. *Biochemistry* 2000;39:10419-10430. doi: 10.1021/bi000365w.
39. Dorfman BZ. The isolation of adenylosuccinate synthetase mutants in yeast by selection for constitutive behavior in pigmented strains. *Genetics* 1969;61:377-389.
40. Creutzburg SCA, Wu WY, Mohanraju P, et al. Good guide, bad guide: spacer sequence-dependent cleavage efficiency of Cas12a. *Nucleic Acids Res* 2020. doi: 10.1093/nar/gkz1240.
41. Guillerez J, Lopez P, Proux F, et al. A mutation in T7 RNA polymerase that facilitates promoter clearance. *PNAS* 2005;102:5958–5963. doi: 10.1073/pnas.0407141102.
42. Yoo J, Kang C. Bacteriophage SP6 RNA polymerase mutants with altered termination efficiency and elongation processivity. *Biomol Eng* 2000;16:191-197. doi: 10.1016/s1389-0344(99)00053-2.
43. Jorgensen ED, Durbin RK, Risman SS, et al. Specific contacts between the bacteriophage T3, T7, and SP6 RNA polymerases and their promoters. *J Biol Chem* 1991;266:645-651.
44. Rong M, Castagna R, McAllister WT. Cloning and purification of bacteriophage K11 RNA polymerase. *Biotechniques* 1999;27:690, 692, 694. doi: 10.2144/99274bm13.
45. Leonetti JP, Mechti N, Degols G, et al. Intracellular distribution of microinjected antisense oligonucleotides. *PNAS* 1991;88:2702-2706. doi: 10.1073/pnas.88.7.2702.
46. Fisher TL, Terhorst T, Cao X, et al. Intracellular disposition and metabolism of fluorescently-labeled unmodified and modified oligonucleotides microinjected into mammalian cells. *Nucleic Acids Res* 1993;21:3857-3865. doi: 10.1093/nar/21.16.3857.
47. Swarts DC, van der Oost J, Jinek M. Structural basis for guide RNA processing and seed-dependent DNA targeting by CRISPR-Cas12a. *Mol Cell* 2017;66:221-233 e224. doi: 10.1016/j.molcel.2017.03.016.
48. Liao C, Slotkowski RA, Achmedov T, et al. The *Francisella novicida* Cas12a is sensitive to the structure downstream of the terminal repeat in CRISPR arrays. *RNA Biol* 2019;16:404-412. doi: 10.1080/15476286.2018.1526537.
49. Gorter de Vries AR, de Groot PA, van den Broek M, et al. CRISPR-Cas9 mediated gene deletions in lager yeast *Saccharomyces pastorianus*. *Microb Cell Fact* 2017;16:222. doi: 10.1186/s12934-017-0835-1.
50. Wagner JC, Platt RJ, Goldfless SJ, et al. Efficient CRISPR-Cas9-mediated genome editing in *Plasmodium falciparum*. *Nat Methods* 2014;11:915-918. doi: 10.1038/nmeth.3063.
51. Lee K, Conboy M, Park HM, et al. Nanoparticle delivery of Cas9 ribonucleoprotein and donor DNA *in vivo* induces homology-directed DNA repair. *Nat Biomed Eng* 2017;1:889-901. doi: 10.1038/s41551-017-0137-2.

52. Juergens H, Varela JA, Gorter de Vries AR, et al. Genome editing in *Kluyveromyces* and *Ogataea* yeasts using a broad-host-range Cas9/gRNA co-expression plasmid. *FEMS Yeast Res* 2018;18. doi: 10.1093/femsyr/foy012.